Biogeosciences, 14, 3831–3849, 2017
https://doi.org/10.5194/bg-14-3831-2017

Biogeosciences Open Access EGU

Alterations in microbial community composition with increasing fCO_2: a mesocosm study in the eastern Baltic Sea

Katharine J. Crawfurd[1], **Santiago Alvarez-Fernandez**[2], **Kristina D. A. Mojica**[3], **Ulf Riebesell**[4], **and Corina P. D. Brussaard**[1,5]

[1]NIOZ Royal Netherlands Institute for Sea Research, Department of Marine Microbiology and Biogeochemistry and Utrecht University, PO Box 59, 1790 AB Den Burg, Texel, the Netherlands
[2]Alfred-Wegener-Institut Helmholtz-Zentrum für Polar- und Meeresforschung, Biologische Anstalt Helgoland, 27498 Helgoland, Germany
[3]Department of Botany and Plant Pathology, Cordley Hall 2082, Oregon State University, Corvallis, Oregon 97331-29052, USA
[4]GEOMAR Helmholtz Centre for Ocean Research Kiel, Biological Oceanography, Düsternbrooker Weg 20, 24105 Kiel, Germany
[5]Aquatic Microbiology, Institute for Biodiversity and Ecosystem Dynamics, University of Amsterdam, PO Box 94248, 1090 GE Amsterdam, the Netherlands

Correspondence to: Katharine J. Crawfurd (kate.crawfurd@gmail.com) and Corina P. D. Brussaard (corina.brussaard@nioz.nl)

Received: 28 November 2015 – Discussion started: 2 February 2016
Revised: 24 June 2017 – Accepted: 3 July 2017 – Published: 29 August 2017

Abstract. Ocean acidification resulting from the uptake of anthropogenic carbon dioxide (CO_2) by the ocean is considered a major threat to marine ecosystems. Here we examined the effects of ocean acidification on microbial community dynamics in the eastern Baltic Sea during the summer of 2012 when inorganic nitrogen and phosphorus were strongly depleted. Large-volume in situ mesocosms were employed to mimic present, future and far future CO_2 scenarios. All six groups of phytoplankton enumerated by flow cytometry (< 20 µm cell diameter) showed distinct trends in net growth and abundance with CO_2 enrichment. The picoeukaryotic phytoplankton groups Pico-I and Pico-II displayed enhanced abundances, whilst Pico-III, *Synechococcus* and the nanoeukaryotic phytoplankton groups were negatively affected by elevated fugacity of CO_2 (fCO_2). Specifically, the numerically dominant eukaryote, Pico-I, demonstrated increases in gross growth rate with increasing fCO_2 sufficient to double its abundance. The dynamics of the prokaryote community closely followed trends in total algal biomass despite differential effects of fCO_2 on algal groups. Similarly, viral abundances corresponded to prokaryotic host population dynamics. Viral lysis and grazing were both important in controlling microbial abundances. Overall our results point to a shift, with increasing fCO_2, towards a more regenerative system with production dominated by small picoeukaryotic phytoplankton.

1 Introduction

Marine phytoplankton are responsible for approximately half of global primary production (Field et al., 1998) with shelf sea communities contributing an average of 15–30 % (Kuliński and Pempkowiak, 2011). Since the industrial revolution, atmospheric carbon dioxide (CO_2) concentrations have increased by nearly 40 % due to anthropogenic emissions, primarily caused by the burning of fossil fuels and deforestation (Doney et al., 2009). Atmospheric CO_2 dissolves in the oceans where it forms carbonic acid that reduces seawater pH, which is a process commonly termed ocean acidification (OA). Currently, along with warming sea surface temperatures and changing light and nutrient conditions, marine ecosystems face unprecedented decreases in ocean pH (Doney et al., 2009; Gruber, 2011). Ocean acid-

ification is considered one of the greatest current threats to marine ecosystems (Turley and Boot, 2010) and has been shown to alter phytoplankton primary production with the direction and magnitude of the responses dependent on community composition (e.g. Hein and Sand-Jensen, 1997; Tortell et al., 2002; Leonardos and Geider, 2005; Engel et al., 2008; Feng et al., 2009; Eberlein et al., 2017). Certain cyanobacteria, including diazotrophs, demonstrate stimulated growth under conditions of elevated CO_2 (Qiu and Gao, 2002; Barcelos e Ramos et al., 2007; Hutchins, et al., 2007; Dutkiewicz et al., 2015). However, no consistent trends have been found for *Synechococcus* (Schulz et al., 2017 and references therein). The responses of diatoms and coccolithophores also appear more variable (Dutkiewicz et al., 2015 and references therein), although coccolithophore calcification seems generally negatively impacted (Meyer and Riebesell, 2015; Riebesell et al., 2017). OA has also been reported to increase the abundances of small-sized photoautotrophic eukaryotes in mesocosm experiments (Engel et al., 2008; Meakin and Wyman, 2011; Brussaard et al., 2013; Schulz et al., 2017).

Recently, data regarding the effects of OA on taxa-specific phytoplankton growth rates were incorporated into a global ecosystem model. The results emphasized that elevated CO_2 concentrations can cause changes in community structure by altering the competitive fitness and thus the competition between phytoplankton groups (Dutkiewicz et al., 2015). Moreover, OA was found to have a greater impact on phytoplankton community size structure, function and biomass than either warming or reduced nutrient supply (Dutkiewicz et al., 2015). Many OA studies have been conducted using single species under controlled laboratory conditions and therefore cannot account for intrinsic community interactions that occur under natural conditions. Alternatively, larger-volume mesocosm experiments allow for OA manipulation of natural communities, and are more likely to capture and quantify the overall response of the natural ecosystems. To date, the majority of these experiments started under replete nutrient conditions or received nutrient additions (Paul et al., 2015 and references therein). Thus, limited data are available for oligotrophic conditions, which are present in $\sim 75\%$ of the world's oceans (Corno et al., 2007).

Whilst environmental factors, such as temperature, light, nutrient and CO_2 concentrations, regulate gross primary production, loss factors determine the fate of this photosynthetically fixed carbon. Grazing, sinking and viral lysis affect the cycling of elements in different manners, i.e. transferred to higher trophic levels through grazing, carbon sequestration in deep waters and sediments, and cellular content release by viral lysis (Wilhelm and Suttle, 1999; Brussaard et al., 2005). Released detrital and dissolved organic matter (DOM) is quickly utilized by heterotrophic bacteria, thereby stimulating activity within the microbial loop (Brussaard et al., 2008; Lønborg et al., 2013; Sheik et al., 2014; Middelboe and Lyck, 2002). Consequently, bacteria may be affected indirectly by OA through changes in the quality and/or quantity of DOM (Weinbauer et al., 2011). Viral lysis has been found to be as important as microzooplankton grazing to the mortality of natural bacterioplankton and phytoplankton (Weinbauer, 2004; Baudoux et al., 2006; Evans and Brussaard, 2012; Mojica et al., 2016). Thus far, most studies examining the effects of OA on microzooplankton abundance and/or grazing have found little or no direct effect (Suffrian et al., 2008; Rose et al., 2009; Aberle et al., 2013; Brussaard et al., 2013; Niehoff et al., 2013). To our knowledge, no viral lysis rates have been reported for natural phytoplankton communities under conditions of OA. A few studies have inferred rates based on changes in viral abundances under enhanced CO_2, but the results are inconsistent (Larsen et al., 2008; Brussaard et al., 2013). Therefore, the effect of OA on the relative share of these key loss processes is still understudied for most ecosystems.

Here we report on the temporal dynamics of microbes (phytoplankton, prokaryotes and viruses) under the influence of enhanced CO_2 concentrations in the low-salinity (around 5.7) Baltic Sea. Using large mesocosms with in situ light and temperature conditions, the pelagic ecosystem was exposed to a range of increasing CO_2 concentrations from ambient to future and far future concentrations. The study was performed during the summer in the Baltic Sea near Tvärminne when conditions were oligotrophic. Our data show that over the 43-day experiment, enhanced CO_2 concentrations elicited distinct shifts in the microbial community, most notably an increase in the net growth of small picoeukaryotic phytoplankton.

2 Materials and methods

2.1 Study site and experimental set-up

The present study was conducted in the Tvärminne Storfjärden (59°51.5′ N, 23°15.5′ E) between 14 June and 7 August 2012. Nine mesocosms, each enclosing $\sim 55\,m^3$ of water, were moored in a square arrangement at a site with a water depth of approximately 30 m. The mesocosms consisted of open-ended polyurethane bags 2 m in diameter and 18.5 m in length mounted onto floating frames covered at each end with a 3 mm mesh. Initially, the mesocosms were kept open for 5 days to allow for rinsing and water exchange while excluding large organisms from entering with the 3 mm mesh. During this time, the bags were positioned such that the tops were submerged 0.5 m below the water surface and the bottoms reached down to 17 m of depth in the water column. Photosynthetically active radiation (PAR) transparent plastic hoods (open on the side) prevented rain and bird droppings from entering the mesocosms, which would affect salinity and nutrients, respectively. Five days before the CO_2 treatment was to begin, the water column of the mesocosms was isolated from the influence of the surrounding water. To do

Table 1. The fCO_2 concentrations (µatm) averaged over the duration of the experiment (following CO_2 addition) and subsequent classification as low, intermediate or high. Mesocosms sampled for mortality assays are denoted by an asterisk. The symbols and colours are used throughout this paper and the corresponding articles in this issue.

Mesocosm	M1*	M5	M7	M6	M3*	M8
CO_2 level	Low	Low	Intermediate	Intermediate	High	High
Mean fCO_2 (µatm) days 1–43	365	368	497	821	1007	1231
Symbol						

so, the 3 mm mesh was removed and sediment traps (2 m long) were attached to close off the bottom of the mesocosms. The top ends of the bags were raised and secured to the frame 1.5 m above the water surface to prevent water from entering via wave action. The mesocosms were then bubbled with compressed air for 3.5 min to remove salinity gradients and ensure that the water body was fully homogeneous.

The present paper includes results from only six of the original mesocosms due to the unfortunate loss of three mesocosms, which were compromised by leakage. The mean fugacity of CO_2 (fCO_2) during the experiment, i.e. days 1–43, for the individual mesocosms were as follows: M1, 365 µatm; M3, 1007 µatm; M5, 368 µatm; M6, 821 µatm; M7, 497 µatm; M8, 1231 µatm (Table 1). The gradient of non-replicated fCO_2 in the present study (as opposed to a smaller number of replicated treatment levels) was selected as a balance between the necessary but manageable number of mesocosms and to minimize the impact of the high loss potential for the mesocosms to successfully address the underlying questions of the study (Schulz and Riebesell, 2013). Moreover, it maximizes the potential of identifying a threshold fCO_2 level concentration if present (by allowing for a larger number of treatment levels). Carbon dioxide manipulation was carried out in four steps and took place between days 0 and 4 until the target fCO_2 was reached. The initial fCO_2 was 240 µatm. For fCO_2 manipulations, 50 µm filtered natural seawater was saturated with CO_2 and then injected evenly throughout the depth of the mesocosms as described by Riebesell et al. (2013). Two mesocosms functioned as controls and were treated in a similar manner using only filtered seawater. On day 15, a supplementary fCO_2 addition was made to the top 7 m of mesocosms numbered 3, 6 and 8 to replace CO_2 lost due to outgassing (Paul et al., 2015; Spilling et al., 2016). Throughout this study we refer to fCO_2, which accounts for the nonideal behaviour of CO_2 gas and is considered the standard measurement required for gas exchange (Pfeil et al., 2013).

Initial nutrient concentrations were 0.05, 0.15, 6.2 and 0.2 µmol L^{-1} for nitrate, phosphate, silicate and ammonium, respectively. Nutrient concentrations remained low for the duration of the experiment (Paul et al., 2015; this issue) and no nutrients were added. Salinity was relatively constant around 5.7. Temperature was more variable; on average temperature within the mesocosms (0–17 m) increased from ∼ 8 °C to a maximum on day 15 of ∼ 15 °C and then decreased again to ∼ 8 °C by day 30. For further details of the experimental set-up, carbonate chemistry dynamics and nutrient concentrations throughout the experiment we refer to the general overview paper by Paul et al. (2015).

Collective sampling was performed every morning using depth-integrated water samplers (IWS; Hydro-Bios, Kiel). These sampling devices were gently lowered through the water column collecting ∼ 5 L of water gradually between 0 and 10 m (top) or 0 and 17 m (whole water column). Water was collected from all mesocosms and the surrounding water. Subsamples were obtained for the enumeration of phytoplankton, prokaryotes and viruses. Samples for viral lysis and grazing experiments were taken from 5 m of depth using a gentle vacuum-driven pump system. Samples were protected against sunlight and warming by thick black plastic bags containing wet ice. Samples were processed at in situ temperature (representative of 5 m of depth) under dim light and handled using nitrile gloves. As viral lysis and grazing rates were determined from samples taken from 5 m of depth, the samples for microbial abundances reported here were taken from the top 10 m integrated samples.

The experimental period has been divided into four phases based on major physical and biological changes (Paul et al., 2015): Phase 0 before CO_2 addition (days −5 to 0), Phase I (days 1–16), Phase II (days 17–30) and Phase III (days 31–43). Throughout this paper, the data are presented using three colours (blue, grey and red), representing low (mesocosms M1 and M5), intermediate (M6 and M7) and high (M3 and M8) fCO_2 levels (Table 1).

2.2 Microbial abundances

Microbes were enumerated using a Becton Dickinson FACSCalibur flow cytometer (FCM) equipped with a 488 nm argon laser. The samples were stored on wet ice and in the dark until counting. The photoautotrophic cells (< 20 µm) were counted directly using fresh seawater and were discriminated by their autofluorescent pigments (Marie et al., 1999). Six phytoplankton clusters were differentiated based on the bivariant plots of either chlorophyll (red autofluorescence) or phycoerythrin (orange autofluorescence for *Synechococcus* and Pico-III) against side scatter. The size of the different phytoplankton clusters was determined by gentle fil-

tration through 25 mm diameter polycarbonate filters (Whatman) with a range of pore sizes (12, 10, 8, 5, 3, 2, 1 and 0.8 µm) according to Veldhuis and Kraay (2004). Average cell sizes for the different phytoplankton groups were 1, 1, 3, 2.9, 5.2 and 8.8 µm in diameter for the prokaryotic cyanobacteria *Synechococcus* spp. (SYN), picoeukaryotic phytoplankton I, II and III (Pico-I–III) and nanoeukaryotic phytoplankton I and II (Nano-I, Nano-II), respectively. Pico-III was discriminated from Pico-II (comparable average cell size) by a higher orange autofluorescence signature, potentially representing small-sized cryptophytes (Klaveness, 1989) or, alternatively, large single cells or microcolonies of *Synechococcus* (Haverkamp et al., 2009). The cyanobacterial species *Prochlorococcus* spp. were not observed during this experiment. Counts were converted to cellular carbon by assuming a spherical shape equivalent to the average cell diameters determined from size fractionations and applying conversion factors of 237 fg C µm^{-3} (Worden et al., 2004) and 196.5 fg C µm^{-3} (Garrison et al., 2000) for pico- and nano-sized plankton, respectively. Microbial net growth and loss rates were derived from exponential regressions of changes in the cell abundances over time.

Abundances of prokaryotes and viruses were determined from 0.5 % glutaraldehyde fixed, flash-frozen (−80 °C) samples according to Marie et al. (1999) and Brussaard (2004). The prokaryotes include heterotrophic bacteria, archaea and unicellular cyanobacteria, the latter accounting for a maximal 10 % of the total abundance in our samples as indicated by their autofluorescence. Thawed samples were diluted with sterile autoclaved Tris-EDTA buffer (10 mM Tris-HCl and 1 mM EDTA; pH 8.2; Mojica et al., 2014) and stained with the green fluorescent nucleic acid-specific dye SYBR Green I (Invitrogen Inc.) to a final concentration of the commercial stock of 1.0×10^{-4} (for prokaryotes) or 0.5×10^{-4} (for viruses). Virus samples were stained at 80 °C for 10 min and then allowed to cool for 5 min at room temperature in the dark. Prokaryotes were stained for 15 min at room temperature in the dark (Brussaard, 2004). Prokaryotes and viruses were discriminated in bivariate scatter plots of green fluorescence versus side scatter. Final counts were corrected for blanks prepared and analysed in a similar manner as the samples. Two groups of prokaryotes were identified by their stained nucleic acid fluorescence, referred here on as low (LNA) and high (HNA) fluorescence prokaryotes.

2.3 Viral lysis and grazing

Microzooplankton grazing and viral lysis of phytoplankton was determined using the modified dilution assay based on reducing grazing and viral lysis mortality pressure in a serial manner allowing for increased phytoplankton growth (over the incubation period) with dilution (Mojica et al., 2016). Two dilution series were created in clear 1.2 L polycarbonate bottles by gently mixing 200 µm sieved whole seawater with either 0.45 µm filtered seawater (i.e. microzooplankton grazers removed) or 30 kDa filtered seawater (i.e. grazers and viruses removed) to final dilutions of 20, 40, 70 and 100 %. The 0.45 µm filtrate was produced by gravity filtration of 200 µm mesh sieved seawater through a 0.45 µm Sartopore capsule filter. The 30 kDa ultrafiltrate was produced by tangential flow filtration of 200 µm pre-sieved seawater using a 30 kDa Vivaflow 200 PES membrane tangential flow cartridge (Vivascience). All treatments were performed in triplicate. Bottles were suspended next to the mesocosms in small cages at 5 m of depth for 24 h. Subsamples were taken at 0 and 24 h, and phytoplankton abundances of the grazing series (0.45 µm diluent) were enumerated by flow cytometry. Due to time constraints, the majority of the samples of the 30 kDa series were fixed with 1 % (final concentration) formaldehyde : hexamine solution (18 % v/v : 10 % w/v) for 30 min at 4 °C, flash-frozen in liquid nitrogen and stored at −80 °C until flow cytometry analysis in the home laboratory. Fixation had no significant effect (Student's t tests; p value > 0.05) as tested periodically against fresh samples. The modified dilution assay was only run for mesocosms 1 (low fCO_2) and 3 (high fCO_2) due to the logistics of handling times. Experiments were performed until day 31. Grazing rates and the combined rate of grazing and viral lysis were estimated from the slope of a regression of phytoplankton apparent growth versus dilution of the 0.45 µm and 30 kDa series, respectively. A significant difference between the two regression coefficients (as tested by analysis of covariance) indicated a significant viral lysis rate. Phytoplankton gross growth rate, in the absence of grazing and viral lysis, was derived from the y-intercept of the 30 kDa series regression. Similarly, significant differences between mesocosms M1 and M3 (low and high fCO_2) were determined through an analysis of covariance of the dilution series for the two mesocosms. A significance threshold of 0.05 was used, and significance is denoted throughout the paper by an asterisk (*). Occasionally, the regression of apparent growth rate versus fraction of natural water resulted in a positive slope (thus no reduction in mortality with dilution). In addition, very low phytoplankton abundances can also prohibit the statistical significance of results. Under such conditions dilution experiments were deemed unsuccessful (for limitations of the modified dilution method, see Baudoux et al., 2006; Kimmance and Brussaard, 2010; Stoecker et al., 2015).

Viral lysis of prokaryotes was determined according to the viral production assay (Wilhelm et al., 2002; Winget et al., 2005). After reduction of the natural virus concentration, new virus production by the natural bacterial community is sampled and tracked over time (24 h). Free viruses were reduced from a 300 mL sample of whole water by recirculation over a 0.2 µm pore size polyether sulfone membrane (PES) tangential flow filter (Vivaflow 50; Vivascience) at a filtrate expulsion rate of 40 mL min^{-1}. The concentrated sample was then reconstituted to the original volume using virus-free seawater. This process was repeated a total of three times to gradually wash away viruses. After the final recon-

stitution, 50 mL aliquots were distributed into six polycarbonate tubes. Mitomycin C (Sigma-Aldrich; final concentration 1 µg mL^{-1}; maintained at 4 °C), which induces lysogenic bacteria (Weinbauer and Suttle, 1996) was added to a second series of triplicate samples for each mesocosm. A third series of incubations with 0.2 µm filtered samples was used as a control for viral loss (e.g. viruses adhering to the tube walls) and showed no significant loss of free viruses during the incubations. At the start of the experiment, 1 mL subsamples were immediately removed from each tube and fixed as previously described for viral and bacterial abundance. The samples were dark incubated at in situ temperature and 1 mL subsamples were taken at 3, 6, 9, 12 and 24 h. Virus production was determined from linear regression of viral abundance over time. Viral production due to induction of lysogeny was calculated as the difference between production in the unamended samples and the production of samples to which mitomycin C was added. Although mortality experiments were initially planned to be employed for mesocosms 1, 2 and 3 representing low, mid and high fCO_2 conditions, mesocosm 2 was compromised due to leakage. Additionally, due to logistical reasons assays were only performed until day 21.

To determine grazing rates on prokaryotes, fluorescently labelled bacteria (FLBs) were prepared from enriched natural bacterial assemblages (originating from the North Sea) labelled with 5-([4,6-dichlorotriazin-2-yl]amino)fluorescein (DTAF 36565; Sigma-Aldrich; 40 µg mL^{-1}) according to Sherr et al. (1993). Frozen ampoules of FLB (1–5 % of total bacterial abundance) were added to triplicate 1 L incubation bottles containing whole water gently passed through 200 µm mesh. Samples of 20 mL were taken immediately after addition (0 h) and the headspace was removed by gently squeezing air from the bottle. The 1 L bottles were incubated on a slow turning wheel (1 rpm) at in situ light and temperature conditions (representative of 5 m of depth) for 24 h. Sampling was repeated after 24 h. All samples were fixed to a 1 % final concentration of gluteraldehyde (0.2 µm filtered; 25 % EM-grade), stained (in the dark for 30 min at 4 °C) with 4',6-diamidino-2-phenylindole dihydrochloride (DAPI) solution (0.2 µm filtered; Acrodisc® 25 mm syringe filters; Pall Life Sciences; 2 µg mL^{-1} final concentration; Sherr et al., 1993) and filtered onto 25 mm, 0.2 µm black polycarbonate filters (GE Healthcare Life Sciences). Filters were then mounted on microscopic slides and stored at −20 °C until analysis. FLBs present on a $\sim 0.75\,mm^2$ area were counted using a Zeiss Axioplan 2 microscope. Grazing (µd^{-1}) was measured according to $N_{T24} = N_{T0} \cdot e^{-\mu t}$, where N_{T24} and N_{T0} are the number of FLBs present at 24 and 0 h, respectively.

2.4 Statistics

Non-metric multidimensional scaling (NMDS) was used to follow microbial community development in each mesocosm over the experimental period. NMDS is an ordination technique which represents the dissimilarities obtained from an abundance data matrix in a two-dimensional space (Legendre and Legendre, 1998). In this case, the data matrix was comprised of abundance data for each phytoplankton group in each mesocosm for every day of sampling. The treatment effect was assessed by an analysis of similarity (ANOSIM; Clarke, 1993) and inspection of the NMDS biplot. ANOSIM compares the mean of ranked dissimilarities in mesocosms between fCO_2 treatments (low: 1, 5, 7; high: 6, 3, 8) to the mean of ranked dissimilarities within treatments per phase. The NMDS plots allowed divergence periods in the development and community composition between treatments to be visually assessed (period 1 from days 3–13 and period 2 from days 16–24). The net growth rates of each of the different microbial groups were calculated for these identified divergence periods. Relationships between net growth rates and peak cell abundances with fCO_2 were evaluated by linear regression against the average fCO_2 per mesocosm during each period or peak day. A generalized linear model was used to test the relationship between prokaryote abundance and carbon biomass with an ARMA correlation structure of order 3 to account for temporal autocorrelation. The model fulfilled all assumptions, such as homoscedasticity and avoiding autocorrelation of the residuals (Zuur et al., 2007). A significance threshold of $p \leq 0.05$ was used, and significance is denoted by an asterisk (*). All analyses were performed using the statistical software program R with the packages nlme (Pinheiro et al., 2017) and vegan (Oksanen et al., 2017; R core Team, 2017). Where averages of low and high mesocosm abundance data are reported, the values represent the average of mesocosms 1, 5 and 7 (mean fCO_2 365–497 µatm) and 6, 3 and 8 (821–1231 µatm).

3 Results

3.1 Total phytoplankton dynamics in response to CO_2 enrichment

During Phase 0, low variability in phytoplankton abundances in the different mesocosms ($1.5 \pm 0.05 \times 10^5$ mL^{-1}) indicated good replicability of initial conditions prior to CO_2 manipulation (Fig. 1). This was further supported by the high similarity between microbial communities in the different mesocosms as indicated by the tight clustering of points in the NMDS plot during this period (Fig. 2). During Phase 0, the phytoplankton community (< 20 µm) was dominated by pico-sized autotrophs, with the prokaryotic cyanobacteria *Synechococcus* (SYN) and Pico-I accounting for 69 and 27 % of total phytoplankton abundance, respectively. After CO_2 addition, there were two primary peaks in phytoplankton, which occurred on day 4 in Phase I and day 24 in Phase II (Fig. 1a). The phytoplankton community became significantly different over time in the different treatments (ANOSIM, $p = 0.01$; Fig. 2). Two periods

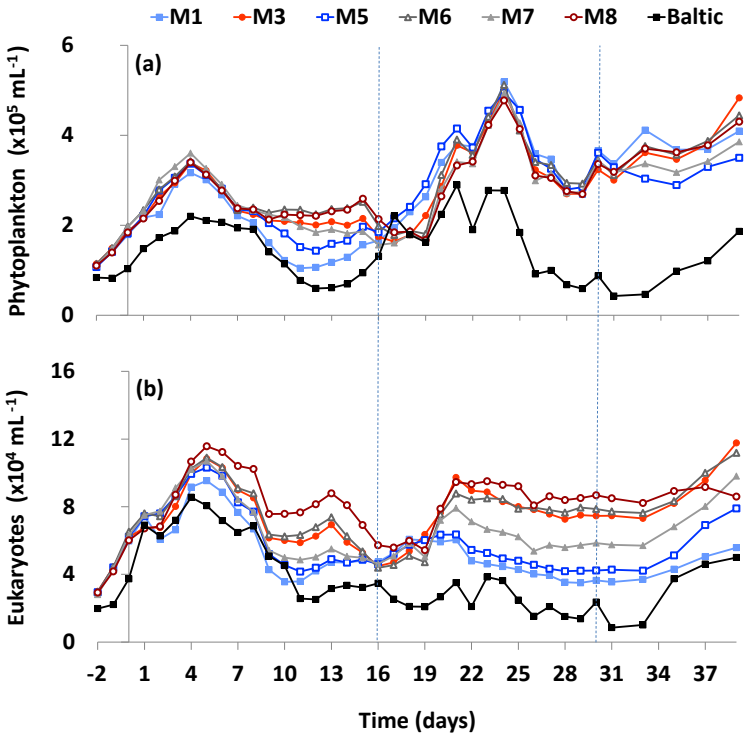

Figure 1. (a) Time series plot of depth-integrated (0.3–10 m) total phytoplankton abundance (< 20 µm) and **(b)** total eukaryotic phytoplankton abundance for each mesocosm and the surrounding waters (Baltic). Dotted lines indicate the end of Phase I and the end of Phase II. Colours and symbols represent the different mesocosms and are consistent throughout the paper. Mean fCO_2 during the experiment (days 1–43): M1, 365 µatm; M3, 1007 µatm; M5, 368 µatm; M6, 821 µatm; M7, 497 µatm; M8, 1231 µatm.

were identified based on their divergence (Fig. 2). The first (NMDS-based period 1) followed the initial peak in abundance (days 3–13) with the highest abundances occurring in the elevated CO_2 mesocosms (Fig. 1a). During the second period (NMDS-based period 2; days 16–24), abundances were higher in the low fCO_2 mesocosms (Fig. 1a). In general the NMDS plot shows that throughout the experiment, mesocosm M1 followed the same basic trajectory as mesocosms M5 and M7, whilst mesocosm M3 followed M6 and M8 (Fig. 2). Thus, the two mesocosms (representing high and low fCO_2 treatments) deviated from each other during Phase I and were clearly separated during Phases II and III (Fig. 2).

Phytoplankton abundances in the surrounding water started to differ from the mesocosms during Phase 0 (on average 44 % lower), which was primarily due to lower abundances of SYN. This effect was seen from day −1 prior to CO_2 addition but following bubbling with compressed air (day −5). On day 15, a deep mixing event occurred as a result of storm conditions (with consequent alterations in temperature and salinity). As a result phytoplankton abundances in the surrounding open water diverged more strongly from the mesocosms but remained similar in their dynamics (Fig. 3). Microbial abundances in the 0–17 m samples were slightly lower but showed very similar dynamics to those in the 0–10 m samples (Fig. S1 in the Supplement).

3.1.1 Synechococcus

The prokaryotic cyanobacteria *Synechococcus* (SYN) accounted for the majority of total abundance, i.e. 74 % averaged across all mesocosms over the experimental period. Abundances of SYN showed distinct variability between the different CO_2 treatments,starting on day 7, with the low CO_2 mesocosms exhibiting nearly 20 % lower abundances between days 11 and 15 compared to high fCO_2 mesocosms (Fig. 3a). SYN net growth rates during days 3–13 (NMDS-based period 1) were positively correlated with CO_2 ($p = 0.10$, $R^2 = 0.53$; Table 2, Fig. S2a). One explanation for higher net growth rates at elevated CO_2 could be the significantly ($p < 0.05$) higher grazing rate in the low fCO_2 mesocosm M1 (0.56 d^{-1}) compared to the high fCO_2 M3 (0.27 d^{-1}) as measured on day 10 (Fig. 4a). After day 16, SYN abundances increased in all mesocosms, and during this period (days 16–24) net growth rates had a significant negative correlation with fCO_2 ($p = 0.05$, $R^2 = 0.63$; Figs. 3a and S3a, Table 2). Consequently, the net increase in SYN abundances during this period was on average 20 % higher at low fCO_2 compared to high fCO_2. This corresponded

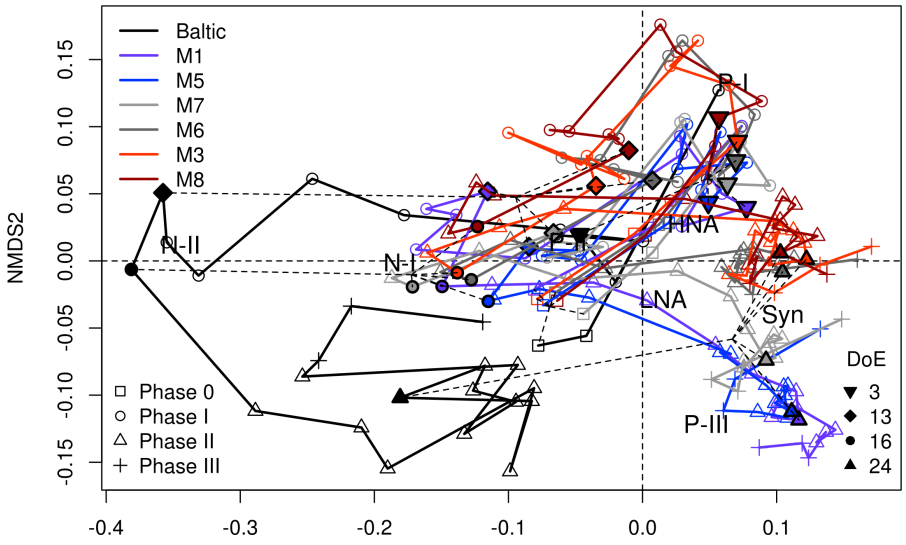

Figure 2. Non-metric multidimensional scaling (NMDS) ordination plot of microbial community development in each mesocosm and the surrounding waters (Baltic) over the experimental period. Phases are indicated by different open symbols. Days of experiment (DoE) when communities separate (3, 13, 16 and 24) are indicated by different closed symbols. Phytoplankton groups are denoted as SYN (Syn), Pico-I (P-I), Pico-II (P-II), Pico-III (P-III), Nano-I (N-I), Nano-II (N-II), low NA prokaryotes (LNA) and high NA prokaryotes (HNA).

to higher total loss rates in high fCO_2 treatments measured on day 17 (0.33 vs. 0.17 d^{-1} for M3 and M1, respectively; Fig. 4a). The higher net growth most likely led to the peak in SYN abundance observed on day 24 (maximum 4.7×10^5 mL^{-1}), which was negatively correlated with fCO_2 ($p = 0.01$, $R^2 = 0.80$; Table 3, Fig. S4a). After this period (days 24–28), SYN abundances declined at comparable rates in the different mesocosms irrespective of fCO_2 (Fig. 3a). Abundances in the low fCO_2 mesocosms remained higher into Phase III (Fig. 3a). SYN abundances in the surrounding water were generally lower than in the mesocosms, with the exception of days 17–21.

3.1.2 Picoeukaryotes

In contrast to the prokaryotic photoautotrophs, the eukaryotic phytoplankton community showed a strong positive response to elevated fCO_2 (Fig. 1b). Pico-I was the numerically dominant group of eukaryotic phytoplankton, accounting for an average 21–26 % of total phytoplankton abundances. Net growth rates leading up to the first peak in abundance (from days 1 to 5) had a strong positive correlation with fCO_2 ($p < 0.01$, $R^2 = 0.90$; Figs. 3b and S5a, Table 3). Accordingly, the peak on day 5 (maximum 1.1×10^5 mL^{-1}; Fig. 3b) was also correlated positively with fCO_2 ($p = 0.01$, $R^2 = 0.81$; Table 3, Fig. S4b). During Phase I from days 3 to 13 (i.e. NMDS-based period 1), net growth rates of Pico-I remained positively correlated with CO_2 concentration ($p = 0.01$, $R^2 = 0.80$; Table 2, Fig. S2b). However, during this period there was also a decline in abundance (days 5–9; $p < 0.01$, $R^2 = 0.89$; Table 3, Fig. S5b) with 23 % more cells lost in the low fCO_2 mesocosms. Accordingly, following this period, gross growth rate was significantly higher in the high fCO_2 mesocosm M3 compared to the low fCO_2 mesocosm M1 (day 10, $p < 0.05$; Fig. 4b). Pico-I abundances in the surrounding open water started to deviate from the mesocosms after day 10 and were on average around half that of the low fCO_2 mesocosms (Fig. 3b). Following a brief increase (occurring between days 11 and 13) correlated with fCO_2 ($p < 0.01$, $R^2 = 0.94$; Table 3, Fig. S4c), abundances declined sharply between days 13 and 16 (Fig. 3b), coincid-

Table 2. The fit (R^2) and significance (p value) of linear regressions applied to assess the relationship between net growth rate and temporally averaged fCO_2 for the different microbial groups distinguished by flow cytometry. The results presented are for two periods distinguished from NMDS analysis: NMDS-based period 1 (days 3–13) and 2 (days 16–24). A significance level of $p \leq 0.05$ was taken and significant results are shown in bold.

Phytoplankton group	NMDS period 1 (days 3–13)		NMDS period 2 (days 16–24)	
	p	R^2	p	R^2
SYN	0.10	0.53	**0.05**	**0.63**
Pico-I	**0.01**	**0.80**	**0.05**	**0.64**
Pico-II	0.52	0.11	0.10	0.52
Pico-III	**0.04**	**0.67**	**<0.01**	**0.91**
Nano-I	**0.01**	**0.79**	0.26	0.30
Nano-II	0.20	0.36	0.06	0.61
HNA	**0.05**	**0.64**	0.89	0.00
LNA	**<0.01**	**0.95**	**0.02**	**0.76**

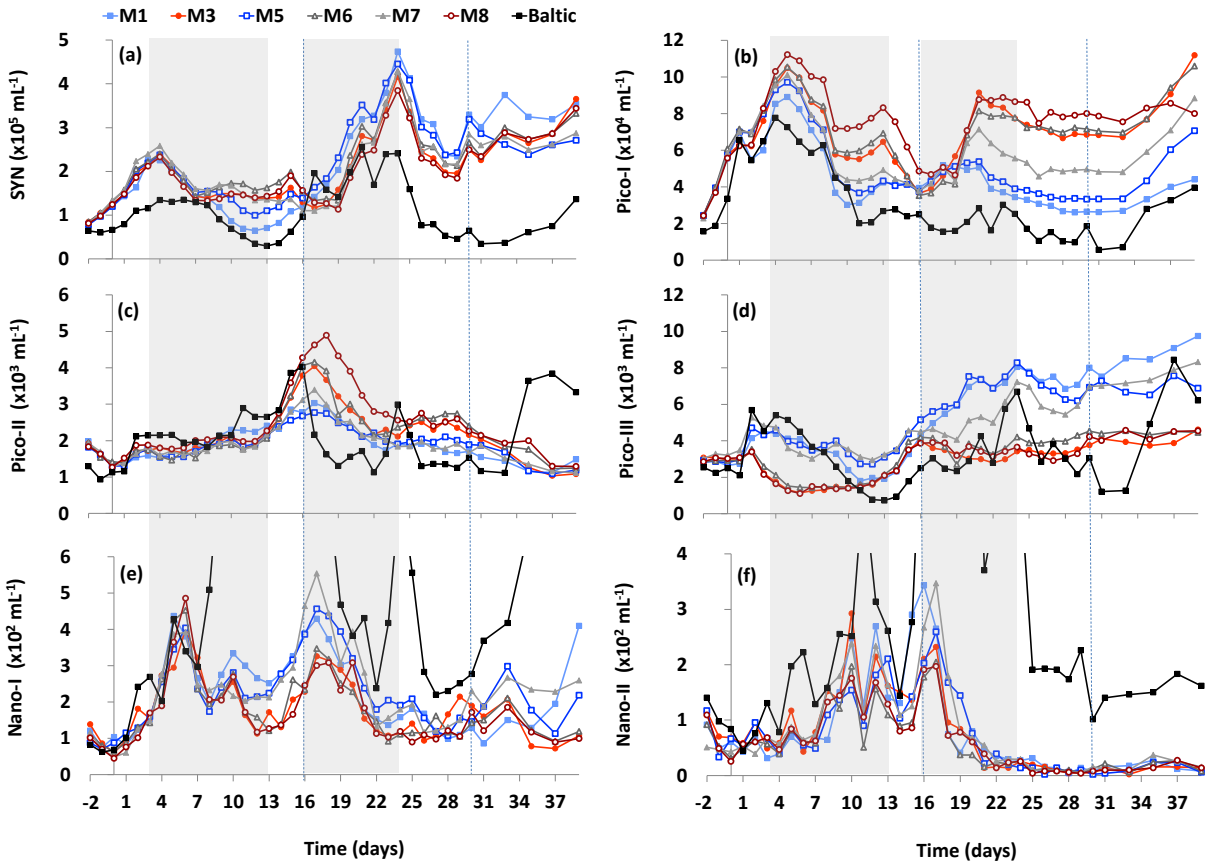

Figure 3. Time series plot of depth-integrated (0.3–10 m) abundances of **(a)** *Synechococcus* (SYN), **(b)** picoeukaryotes I (Pico-I), **(c)** picoeukaryotes II (Pico-II), **(d)** picoeukaryotes III (Pico-III), **(e)** nanoeukaryotes I (Nano-I) and **(f)** nanoeukaryotes II (Nano-II) distinguished by flow cytometric analysis of the microbial community in each mesocosm and the surrounding waters (Baltic). Dotted lines indicate the end of Phase I and the end of Phase II; grey areas indicate NMDS-based periods 1 and 2 during which net growth rates were analysed.

Table 3. The fit (R^2) and significance (p value) of linear regressions used to relate peak abundances and net growth rate with temporally averaged fCO_2 for the different microbial groups distinguished by flow cytometry during specific periods of interest. A significance level of $p \leq 0.05$ was taken and significant results are shown in the table below.

	Peak abundance		Net growth rate	
	p	R^2	p	R^2
SYN day 24	0.01	0.80	–	–
Pico-I day 5	0.01	0.81	–	–
Pico-I day 13	< 0.01	0.94	–	–
Pico-I day 21	0.01	0.84	–	–
Pico-II day 17	< 0.01	0.93	–	–
Pico-III day 24	< 0.01	0.91	–	–
Nano-I day 17	0.04	0.67	–	–
Pico-I days 1–5	–	–	< 0.01	0.90
Pico-I days 5–9	–	–	< 0.01	0.89
Pico-II days 12–17	–	–	0.01	0.82

ing with a significantly higher total mortality rate in the high fCO_2 mesocosm M3 (day 13; Fig. 4b). Viral lysis was a substantial loss factor relative to grazing for this group, comprising an average 45 and 70 % of total losses in M1 and M3, respectively (Table S1). During NMDS-based period 2, net growth rates of Pico-I were significantly higher at high fCO_2 ($p = 0.05$, $R^2 = 0.64$; Table 2, Fig. S3b). By day 21, abundances in the high fCO_2 mesocosms were (on average) ~2-fold higher than at low fCO_2 (maximum abundances 8.7×10^4 and 5.9×10^4 mL^{-1} for high and low fCO_2 mesocosms; $p = 0.01$, $R^2 = 0.84$; Table 3, Fig. S4d). Standing stock of Pico-I remained high in the elevated fCO_2 mesocosms for the remainder of the experiment (7.9×10^4 vs. 4.3×10^4 mL^{-1} on average for high and low fCO_2 mesocosms, respectively; Fig. 3b). Additionally, gross growth rates during this final period were relatively low (0.14 and 0.16 d^{-1} in M1 and M3, respectively) and comparable to total loss rates (averaging 0.13 and 0.10 d^{-1} over days 25–31 for M1 and M3, respectively; Fig. 4b).

Another picoeukaryote group, Pico-II, slowly increased in abundance until day 13, when it increased more rapidly

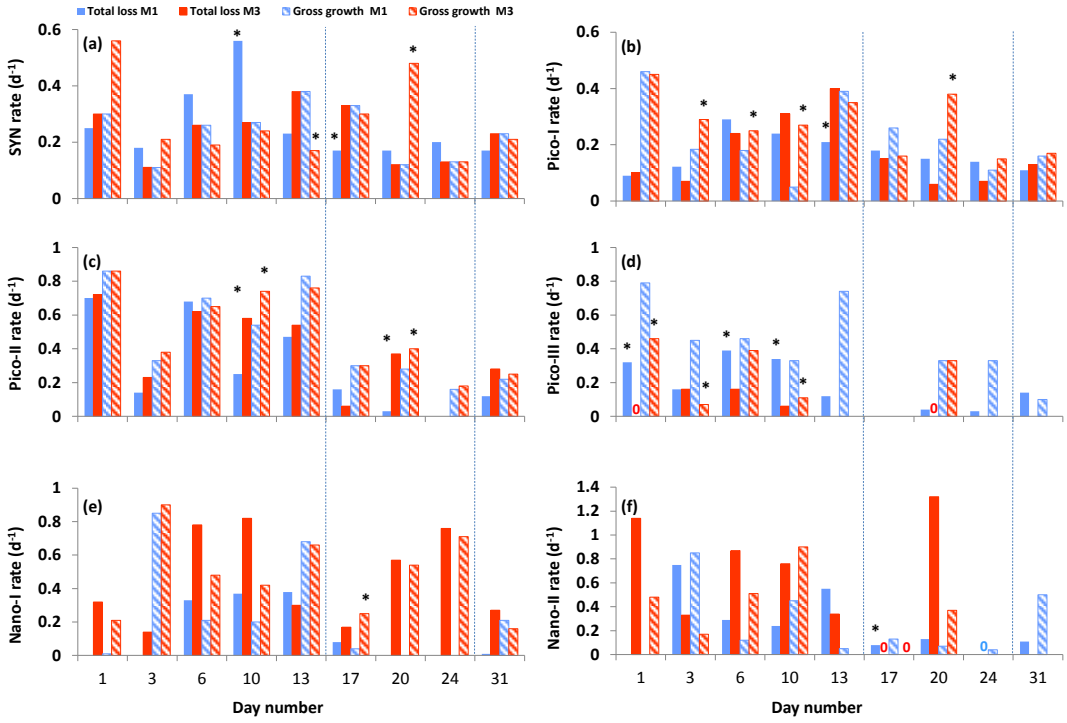

Figure 4. Total mortality rates (i.e. grazing and lysis; solid bars) and gross growth rates (striped bars) d^{-1} of the different phytoplankton groups in mesocosms M1 (blue) and M3 (red) on the day indicated: **(a)** *Synechococcus* (SYN), **(b)** picoeukaryotes I (Pico-I), **(c)** picoeukaryotes II (Pico-II), **(d)** picoeukaryotes III (Pico-III), **(e)** nanoeukaryotes I (Nano-I) and **(f)** nanoeukaryotes II (Nano-II). Significant ($p \leq 0.05$) differences between mesocosms are indicated by an asterisk above the relevant bar (either total loss or gross growth). A coloured zero indicates that a rate of zero was measured in the mesocosm of the corresponding colour; the absence of a bar or zero indicates a failed experiment. Dotted lines indicate the end of Phase I and the end of Phase II.

(Fig. 3c). Gross growth rates measured during Phase I were high (0.69 and 0.72 d^{-1} on average in the low and high fCO_2 mesocosms M1 and M3, respectively; Fig. 4c) and comparable to loss processes (0.46 and 0.58 d^{-1}), indicative of a relatively high turnover rate of production. Overall net growth rates during days 3–13 (NMDS-based period 1) did not correlate with CO_2 ($p = 0.52$, $R^2 = 0.11$; Table 2, Fig. S2c). However, during periods of rapid increases in net growth, abundances were positively correlated with CO_2 concentration (days 12–17; $p = 0.01$, $R^2 = 0.82$; Table 3, Fig. S5c). Accordingly, the peak in abundances of Pico-II on day 17 displayed a distinct positive correlation with fCO_2 ($p < 0.01$, $R^2 = 0.93$; Table 3, Fig. S4e) with maximum abundances of 4.6×10^3 and 3.4×10^3 mL^{-1} for the high and low fCO_2 mesocosms, respectively (Fig. 3c). In M8 (the highest fCO_2 mesocosm), abundances increased for an extra day with the peak occurring on day 18, resulting in an average of 23 % higher abundances. During the decline in the Pico-II peak (days 16–24), net growth rates were negatively correlated with fCO_2 ($p = 0.10$, $R^2 = 0.52$; Table 2, Fig. S3c). Moreover, the rate of decline was faster for the high fCO_2 mesocosms during days 18–21 ($p < 0.01$, $R^2 = 0.85$). The Pico-II abundances in the surrounding water were comparable to the mesocosms during Phases 0 and I, lower during Phase II and higher during Phase III (Fig. 3c).

Pico-III exhibited a short initial increase in abundances in the low fCO_2 treatments, resulting in nearly 2-fold higher abundances at low fCO_2 by day 3 compared to the high fCO_2 treatment (Fig. 3d). After this initial period, net growth rates of this group had a significant positive correlation with fCO_2 (days 3–13; $p = 0.04$, $R^2 = 0.67$; Table 2, Fig. S2d). In general, during Phase I gross growth ($p < 0.01$; days 1, 3, 10; Fig. 4d) and total mortality ($p < 0.05$; days 1, 6, 10; Fig. 4d) were significantly higher in the low fCO_2 mesocosm M1 compared to the high fCO_2 mesocosm M3, resulting in low net growth rates. During Phase II (days 16–24; NMDS-based period 2) the opposite occurred; i.e. net growth rates were negatively correlated with fCO_2 ($p < 0.01$, $R^2 = 0.86$; Table 2, Fig. S3d). Maximum Pico-III abundances (day 24: 4.2×10^3 and 8.3×10^3 mL^{-1} for high and low fCO_2) had a strong negative correlation with fCO_2 ($p < 0.01$, $R^2 = 0.91$; Table 3, Fig. S4f). Pico-III abundances remained noticeably higher in the low fCO_2 mesocosms during Phases II and III (on average 80 %; Fig. 3d). Unfortunately, almost half of the mortality assays in this second half of the experiment failed (see Sect. 2), but the successful assays suggest that losses were minor (< 0.15 d^{-1};

Fig. 4d) and primarily due to grazing, as no significant viral lysis was detected (Table S1).

3.1.3 Nanoeukaryotes

Nano-I showed maximum abundances ($4.3 \pm 0.4 \times 10^2$ mL^{-1}) on day 6 (except M1, which peaked on day 5) independent of fCO_2 ($p = 0.23$, $R^2 = 0.33$; Fig. 3e). There was, however, a negative correlation of net growth rate with fCO_2 during days 3–13 (NMDS-based period 1; $p = 0.01$, $R^2 = 0.79$; Table 2, Fig. S2e). A second major peak in abundance of Nano-I occurred on day 17, with markedly higher numbers in the low fCO_2 mesocosms (4.1×10^2 mL^{-1} compared to 2.4×10^2 mL^{-1} in high fCO_2 mesocosms; $p = 0.04$, $R^2 = 0.67$; Figs. 3e and S4g, Table 3). Total loss rates in the high fCO_2 mesocosm M3 on days 6 and 10 were 2.3-fold higher compared to the low fCO_2 mesocosm M1 (Fig. 4e), which may help to explain this discrepancy in total abundance between low and high fCO_2 mesocosms. Viral lysis accounted for up to 98 % of total losses in the high fCO_2 mesocosm M3 during this period, whilst in M1 viral lysis was only detected on day 13 (Table S1 in the Supplement). Peak abundances (around 5.0×10^2 mL^{-1}) were much lower compared to those in the surrounding waters (max $\sim 2.4 \times 10^3$ mL^{-1}; Figs. 3e and S6a). During Phase II, Nano-I abundances in the surrounding waters displayed rather erratic dynamics compared to those of the mesocosms but converged during certain periods (e.g. days 19–22). No significant relationship was found between net loss rates and fCO_2 for the second NMDS-based period ($p = 0.26$, $R^2 = 0.30$; Table 2, Fig. S3e). At the end of Phase II, abundances were similar in all mesocosms but diverged again during Phase III (days 31–39) due primarily to a negative effect of CO_2 on Nano-I abundances, as depicted in the average 36 % reduction in Nano-I.

The temporal dynamics of Nano-II, the least abundant phytoplankton group analysed in our study, displayed the largest variability (Fig. 3f), perhaps due to the spread of this cluster in flow cytographs (which may indicate that this group represents several different phytoplankton species). No significant relationship was found between net growth rate and fCO_2 for this group for the two NMDS-based periods (Table 2, Figs. S2f and S3f) nor with the peak in abundances on day 17 ($p = 0.13$, $R^2 = 0.46$; Fig. S4h). Moreover, no consistent trend was detected in mortality rates (Fig. 4f). Similar to Nano-I, abundances in the surrounding water were often higher than in the mesocosms (maximum 3.5×10^2 mL^{-1} vs. 1.1×10^4 mL^{-1}, respectively; Figs. 3f and S6b).

3.1.4 Algal carbon biomass

The mean combined biomass of Pico-I and Pico-II showed a strong positive correlation with fCO_2 throughout the experiment ($p < 0.05$, $R^2 = 0.95$; Fig. 5a), an effect already noticeable by day 2. Their biomass in the high fCO_2 mesocosms was, on average 11 % higher than in the low fCO_2 mesocosms between days 10 and 20 and 20 % higher between days 20 and 39. Conversely, the remaining algal groups showed an average 10 % reduction in carbon biomass at enhanced fCO_2 (days 3–39, the sum of SYN, Pico-III, Nano-I and II; $p < 0.01$; Fig. 5b). The most notable response was found for the biomass of Pico-III, which showed an immediate negative response to CO_2 addition (Fig. S7a) and remained on average 29 % lower throughout the study period (days 2–39). For Nano-I and Nano-II the lower carbon biomass only became apparent during the end of Phase I and the beginning of Phase II (days 14–20; Fig. S7b). Due to its small cell size, the numerically dominant SYN accounted for an average of 40 % of total carbon biomass.

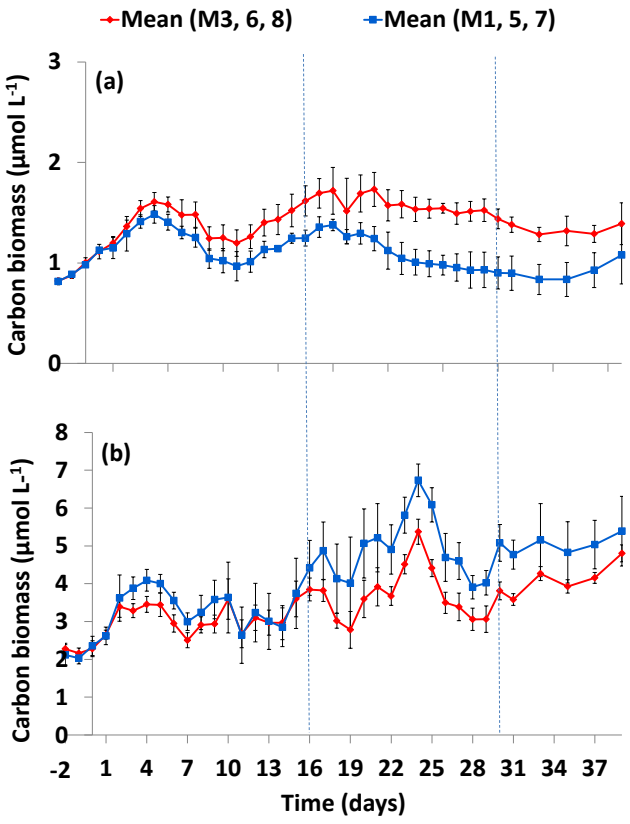

Figure 5. Time series plot of the mean phytoplankton carbon biomass in high fCO_2 (M3, M6, M8; red) and low fCO_2 (M1, M5, M7; blue) mesocosms of **(a)** Pico-I and Pico-II combined and **(b)** SYN, Pico III, Nano-I and Nano-II combined. Error bars represent 1 standard deviation from the mean. Carbon biomass is calculated assuming a spherical diameter equivalent to the mean average cell diameters for each group and conversion factors of 237 fg C µm^{-3} (Worden et al., 2004) and 196.5 fg C µm^{-3} (Garrison et al., 2000) for pico- and nano-sized plankton, respectively. Dotted lines indicate the end of Phase I and the end of Phase II.

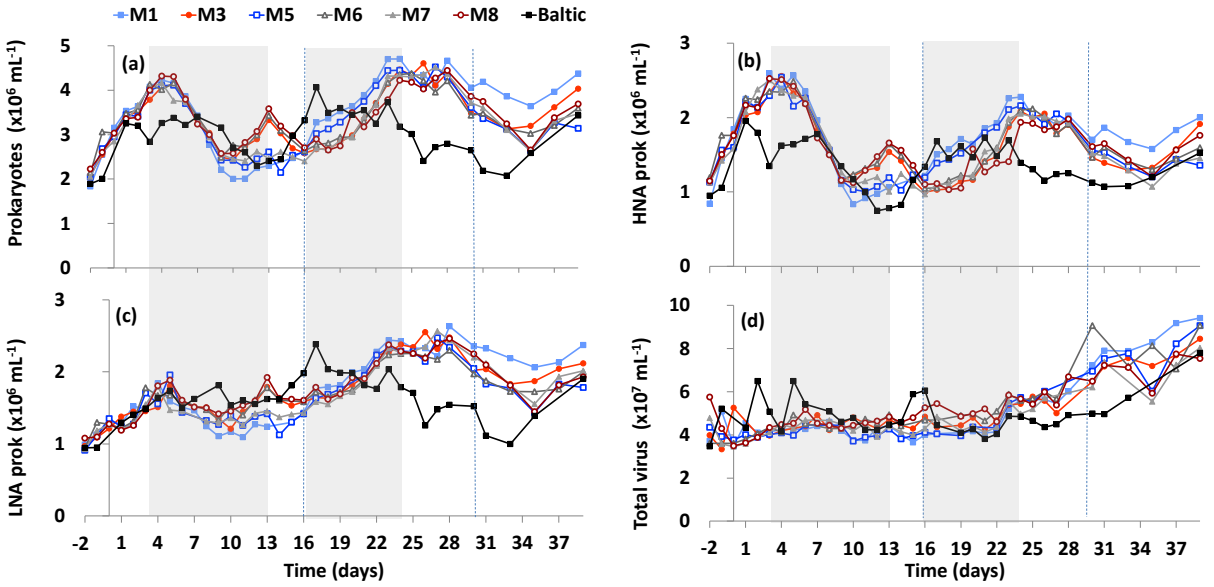

Figure 6. Time series plot of depth-integrated (0.3–10 m) abundances of **(a)** total prokaryotes, **(b)** high fluorescent nucleic acid prokaryote population (HNA), **(c)** low fluorescent nucleic acid prokaryote population (LNA) and **(d)** total virus. Dotted lines indicate the end of Phase I and the end of Phase II; grey areas indicate NMDS-based periods during which net growth rates were analysed.

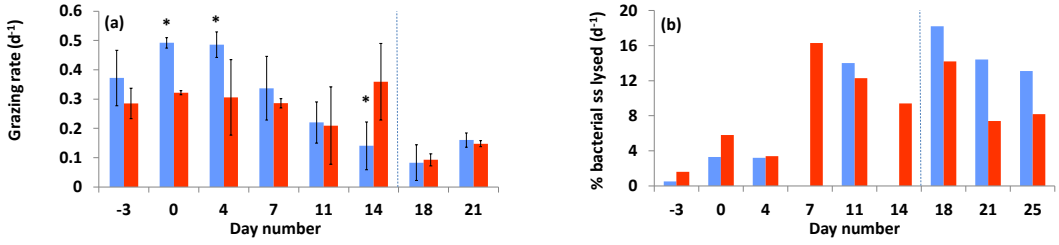

Figure 7. Prokaryote mortality rates: **(a)** total grazing (d^{-1}) and **(b)** viral lysis rates as % of prokaryote standing stock in mesocosms M1 (low fCO_2; blue) and M3 (high fCO_2; red). Grazing rates were determined from fluorescently labelled prey, and viral lysis rates from viral production assays. Error bars represent 1 standard deviation of triplicate assays. Significant ($p \leq 0.05$) differences between mesocosms are indicated by an asterisk. Dotted lines indicate the end of Phase I.

3.2 Prokaryote and virus population dynamics

Prokaryote abundance in the mesocosms was positively related to total algal biomass independent of treatment ($p < 0.05$, $R^2 = 0.33$; Fig. 8) and generally followed total algal biomass (Fig. S7c). The initial increase in total prokaryote abundances occurred during the first few days following the closure of the mesocosms (Fig. 6a). This was primarily due to increases in the HNA prokaryote group (Fig. 6b), which displayed higher net growth rates ($0.22\,d^{-1}$) compared to the LNA prokaryotes ($0.14\,d^{-1}$ on days −3 to 3; Fig. 6c). A similar, albeit somewhat lower, increase was also recorded in the surrounding waters (Fig. 6a). The decline in the first peak in prokaryote abundances coincided with the decay in phytoplankton abundance and biomass (Figs. 1a and S7c). Concurrently the share of viral lysis increased, representing 37–39 % of total mortality on day 11 (Fig. 7b). No measurable rates of lysogeny were found for the prokaryotic community during the experimental period (all phases). From days 10 to 15 prokaryote dynamics (total, HNA and LNA) became noticeably affected by CO_2 concentration with a significant positive correlation between net growth and fCO_2 during Phase I (days 3–13; NMDS-based period 1; Table 2, Fig. S2g and h). In the higher fCO_2 mesocosms, the decline in prokaryote abundance occurring between days 13 and 16 (Fig. 6a) was largely (70 %) due to decreasing HNA prokaryote numbers (Fig. 6b). The grazing was 1.6-fold higher in the high fCO_2 mesocosm M3 compared to M1 (0.36 ± 0.13 and $0.14 \pm 0.08\,d^{-1}$ on day 14; Fig. 7a). At the same time, viral abundance increased in the high fCO_2 mesocosms (Fig. 6d).

During Phase II, prokaryote abundances increased steadily until day 24 (for both HNA and LNA), corresponding to increased algal biomass (Figs. 6 and S7c) and lowered grazing rates (Fig. 7a). Specifically, during days 16–24 (NMDS-

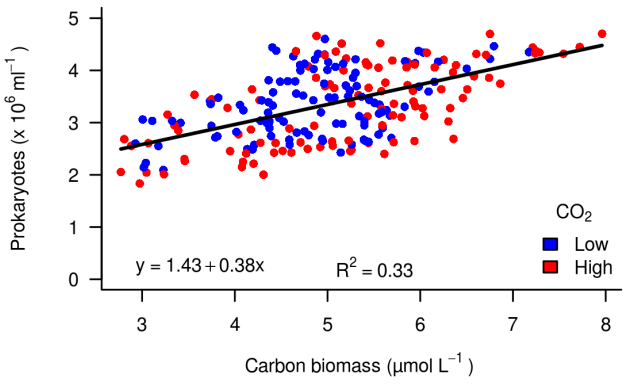

Figure 8. Correlation between total carbon biomass (µmol L^{-1}) and total prokaryote abundance in low fCO_2 mesocosms (M1, M5, M7; blue) and high fCO_2 mesocosms (M3, M6, M8; red) throughout the experiment (days −2 to 39).

based period 2), the HNA prokaryotes showed an average 10 % higher abundances in the low compared to the high fCO_2 mesocosms (Fig. 6b). However, a significant negative correlation of net growth rates and fCO_2 was only found for LNA (Table 2, Fig. S3g and h). No significant differences in loss rates between M1 and M3 were found during Phase II ($p = 0.22$ and $p = 0.46$ on days 18 and 21, respectively; Fig. 7). Halfway through Phase II (day 24), the prokaryote abundance in the surrounding water levelled off (Fig. 6a). Prokaryote abundance ultimately declined during days 28–35 (Fig. 6a), and the net growth of LNA was again negatively correlated with enhanced CO_2 ($p = 0.02$, $R^2 = 0.76$; Table 2, Fig. S3g). Unfortunately, no experimental data on grazing and lysis of prokaryotes are present after day 25. However, viral abundances increased steadily at 2.2×10^6 d^{-1} concomitant with a decline in prokaryote abundance (Fig. 6a and d). There was no significant correlation between viral abundances and fCO_2 during Phases II and III ($p = 0.36$, $R^2 = 0.21$).

4 Discussion

In most experimental mesocosm studies, nutrients have been added to stimulate phytoplankton growth (Schulz et al., 2017); therefore limited data exists for oligotrophic phytoplankton communities. In this study, we describe the impact of increased fCO_2 on the brackish Baltic Sea microbial community during summer (nutrient depleted; Paul et al., 2015). Small-sized phytoplankton numerically dominated the autotrophic community, in particular SYN and Pico-I (both about 1 µm in cell diameter). Our results demonstrate variable effects of fCO_2 manipulation on temporal phytoplankton dynamics, dependent on phytoplankton group. In particular, Pico-I and Pico-II showed significant positive responses, whilst the abundances of Pico-III, SYN and Nano-I were negatively influenced by elevated fCO_2. The impact of OA on the different groups was, at times, a direct consequence of alterations in gross growth rate, whilst overall phytoplankton population dynamics could be explained by the combination of growth and losses. OA effects on community composition in these systems may have consequences on both the food web and biogeochemical cycling.

4.1 Comparison with surrounding waters

During Phase 0, the microbial assemblage showed good replicability among all mesocosms; however, they had already began to deviate from the community in the surrounding waters. This was most likely a consequence of water movement altering the physical conditions and biological composition of the surrounding water body. The dynamic nature of water movement in this region has been shown to alter the entire phytoplankton community several times over within a few months due to fluctuations in nutrient supply, advection, replacement or mixing of water masses and water temperature (Lips and Lips, 2010). Alternatively, the effects of enclosure and the techniques (bubbling) used to ensure a homogenous water column may have stimulated SYN within the mesocosms, which has been found to occur in several mesocosm experiments (Paulino et al., 2008; Gazeau et al., 2017). By Phases II and III, the microbial abundances within the mesocosms were distinctly different from the surrounding waters, with generally fewer SYN and Pico-I and more Nano-I and Nano-II. Our statistical analysis shows that during this time, there was little similarity between the surrounding waters and mesocosms regardless of the CO_2 treatment level. Thus, the deviations during this time were most likely due to an upwelling event in the archipelago (days 17–30; Paul et al., 2015). Cold, nutrient-rich deep water has been shown to upwell during summer with a profound positive influence on ecosystem productivity (Nômmann et al., 1991; Lehmann and Myrberg, 2008). A relaxation from nutrient limitation in vertically stratified waters disproportionately favours larger-sized phytoplankton due to their higher nutrient requirements and lower capacity to compete at low concentrations dictated by their lower surface to volume ratio (Raven, 1998; Veldhuis et al., 2005). Inside the mesocosms, which were isolated from upwelled nutrients, picoeukaryotes dominated similar to a stratified water column. Following this upwelling event, the pH of the surrounding waters dropped from 8.3 to 7.8, a level comparable to the highest CO_2 treatment (M8) on day 32 (Paul et al., 2015). This suggests that other factors contributed to the observed differences between mesocosms and the surrounding water than can be accounted for by CO_2 concentration alone, e.g. nutrients. Alternatively, the magnitude and source of mortality occurring in the surrounding water may have been altered compared to within the mesocosms after such an upwelling event. Although the grazer community in the surrounding waters was not studied during this campaign, it is likely that

the grazing community was completely restructured during the upwelling event (Uitto et al., 1997). It is nonetheless noteworthy that the phytoplankton groups with distinct responses to CO_2 enrichment (either positive or negative) in the low (ambient) fCO_2 mesocosms diverged from those in the surrounding water before the upwelling event occurred.

4.2 Phytoplankton dynamics

Synechococcus showed significantly lower net growth rates and peak abundances at higher fCO_2. Both in laboratory and mesocosm experiments, *Synechococcus* has been reported to have diverse responses to CO_2 with approximately equal accounts of positive (Lu et al., 2006; Schulz et al., 2017), negative (Paulino et al., 2008; Hopkins et al., 2010; Traving et al., 2014,) and insignificant changes (Fu et al., 2007; Lu et al., 2006) in net growth rate with fCO_2. This variable response is probably due, at least in part, to the broad physiological and genetic diversity of this species. In the Gulf of Finland alone, 46 different strains of *Synechococcus* were isolated in July 2004 (Haverkamp et al., 2009). Direct effects on physiology have been implied from laboratory studies. One isolate, a phycoerythrin-rich strain of *Synechococcus* WH7803 (Traving et al., 2014), elicited a negative physiological effect on the growth rate from increased CO_2. This was most likely a consequence of higher sensitivity to the lower pH (Traving et al., 2014) and the cellular cost of maintaining pH homeostasis or, conversely, a direct effect on protein export. Additionally, Lu et al. (2006) reported increased growth rates in a cultured phycocyanin-rich but not a phycoerythrin-rich strain of *Synechococcus*, suggesting that pigments may play some part in defining the direct physiological response within *Synechococcus*. In addition, within natural communities (Paulino et al., 2008; Hopkins et al., 2010; Schulz et al., 2017) variability can also arise from indirect effects, such altering competition with other picoplankton (Paulino et al., 2008). The delay and dampened effect of fCO_2 on SYN abundances within our study was more likely due to indirect effects arising from alterations in food web dynamics than to direct impacts on the physiology of this species. Specifically, significant differences in grazing rates of SYN between M1 and M3 (days 10 and 17, no significant lysis detected) could be responsible for the differing dynamics between the mesocosms at the end of Phase I and the beginning of Phase II.

The gross growth rates of Pico-I were significantly higher ($p < 0.05$) at high fCO_2 compared to the low CO_2 concentrations during the first 10 days of Phase I. Moreover, no differences were detected in the measured loss rates, demonstrating that increases in Pico-I were the due to increases in growth alone. The stimulation of Pico-I by elevated fCO_2 may be due to a stronger reliance on diffusive CO_2 entry compared to larger cells. Model simulations reveal that whilst near-cell CO_2 and pH conditions are close to those of the bulk water for cells $< 5\,\mu m$ in diameter, they diverge as cell diameters increase (Flynn et al., 2012). This is due to the size-dependent thickness of the diffusive boundary layer, which determines the diffusional transport across the boundary layer and to the cell surface (Wolf-Gladrow and Riebesell, 1997; Flynn et al., 2012). It is suggested that larger cells may be more able to cope with fCO_2 variability as their carbon acquisition is more geared towards handling low CO_2 concentrations in their diffusive boundary layer, e.g. by means of active carbon acquisition and bicarbonate utilization (Wolf-Gladrow and Riebesell, 1997; Flynn et al., 2012). Moreover, as the Baltic Sea experiences particularly large seasonal fluctuations in pH and fCO_2 (Jansson et al., 2013) due to the low buffering capacity of the waters, phytoplankton here are expected to have a higher degree of physiological plasticity. Our results agree with previous mesocosm studies, which reported enhanced abundances of picoeukaryotic phytoplankton (Brussaard et al., 2013; Davidson et al, 2016; Schulz et al., 2017), particularly the prasinophyte *Micromonas pusilla* at higher fCO_2 (Engel et al., 2008; Meakin and Wyman, 2011). Furthermore, Schaum et al. (2012) found that 16 ecotypes of *Ostreococcus tauri* (another prasinophyte similar in size to Pico-I) increased in growth rate by 1.4–1.7-fold at 1000 compared to 400 µatm fCO_2. All ecotypes increased their photosynthetic rates, and those with the most plasticity (those most able to vary their photosynthetic rate in response to changes in fCO_2) were more likely to increase in frequency within the community. It is possible that Pico-I cells are adapted to a highly variable carbonate system regime and are able to increase their photosynthetic rate when additional CO_2 is available. This ability would allow them to out-compete other phytoplankton (e.g. nanoeukaryotes in this study) in an environment when nutrients are scarce.

The net growth rates and peak abundances of Pico-II were also positively affected by fCO_2. Gross growth rates were significantly higher at high fCO_2 on only two occasions (days 10 and 20) and were accompanied by high total mortality rates. Pigment analysis suggests that both Pico-I and Pico-II are chlorophytes (Paul et al., 2015) and as such may share a common evolutionary history (Schulz et al., 2017); thus Pico-II may be stimulated by fCO_2 in a similar manner to Pico I. Chlorophytes are found in high numbers at this site throughout the year (Kuosa, 1991), suggesting the ecological relevance of Pico-I and Pico-II in this ecosystem. In addition, Pico-II bloomed exactly when Pico-I declined, which may suggest potential competitive exclusion.

Pico-III showed the most distinct and immediate response to CO_2 addition. The significant reduction in gross growth rates observed during Phase I suggests a direct negative effect of CO_2 on the physiology of these cells. For this group, the lower gross growth rates were matched by lower total mortality rates with increased fCO_2. Although the mean cell size of Pico-III and Pico-II were comparable (2.9 and 2.5 µm, respectively), they showed opposing responses to fCO_2 enrichment (lower Pico-III abundances at high fCO_2). These

differences may arise from taxonomic differences between the two groups. Pico-III displayed relatively high phycoerythrin orange autofluorescence, likely representing small-sized cryptophytes (Klaveness, 1989), although rod-shaped *Synechococcus* up to 2.9 µm in length (isolated from this region; Haverkamp et al., 2009) or *Synechococcus* microcolonies (often only two cells in the Baltic; Motwani and Gorokhove, 2013) cannot be excluded. In agreement with Pico-III response to CO_2 enrichment, Hopkins et al. (2010) reported reduced abundances of small cryptophytes under increased CO_2 in a mesocosm study in a Norwegian fjord near Bergen.

Lastly, the two nanoeukaryotic phytoplankton groups also displayed a negative response to fCO_2 enrichment; Nano-II was the least defined, most likely due to a high taxonomic diversity in this group. Nano-I started to display lower abundances at high fCO_2 during Phase I (after day 10), which was likely the result of greater differences between gross growth and total mortality (compared to low fCO_2). Alternatively, enhanced nutrient competition due to increased abundances of SYN and Pico-I (and later also Pico-II) at elevated fCO_2 may also have contributed to the dampened response of Nano-I in the high fCO_2 mesocosms. The overall decline in Nano-I during Phase II and the sustained low abundances during Phase III may well have been the result of grazing by the increased mesozooplankton abundances during Phase II (Lischka et al., 2017).

4.3 Microbial loop

The strong association of prokaryote abundance with algal biomass, which was present throughout the experiment, suggests that the effect of CO_2 was an indirect consequence of alterations in the availability of phytoplankton carbon. Others have reported a tight coupling of autotrophic and heterotrophic communities at this location, with an estimated 35 % of the total net primary production being utilized directly by bacteria or heterotrophic flagellates (Kuosa and Kivi, 1989), suggesting a highly efficient microbial loop in this ecosystem. In addition to phytoplankton exudation, viral lysis may also contribute to the dissolved organic carbon pool (Wilhelm and Suttle, 1999; Brussaard et al., 2005; Lønborg et al., 2013). We calculated that viral lysis of phytoplankton between days 9 and 13 resulted in the release of 1.3 and 13.1 ng C mL^{-1} for M1 and M3, respectively. Assuming a bacterial growth efficiency of 30 % and cellular carbon conversion of 7 fg C $cell^{-1}$ (Hornick et al., 2017), we estimate that the organic carbon required to support bacterial dynamics during this period (taking into account the net growth and loss rates) was 2.9 and 11.5 ng C mL^{-1} in the low and high fCO_2 mesocosms M1 and M3, respectively. These results suggest that viral lysis of phytoplankton was an important source of organic carbon for the bacterial community. Our results are consistent with bacterial–phytoplankton coupling during this eastern Baltic Sea mesocosm study (Hornick et al., 2017) and agree with earlier work on summer carbon flow in the northern Baltic Sea showing that prokaryotic growth was largely supported by recycled carbon (Uitto et al., 1997). The average net growth rates of the prokaryotes during the first period of increase in Phases 0 and I (0.2 d^{-1}) were comparable to rates reported for this region (Kuosa, 1991). In order to sustain the concomitant daily mortality (between 0.3 and 0.5 d^{-1}) measured during our study, prokaryotic gross growth rates must have been close to one doubling a day (0.5–0.7 d^{-1}). During Phase I, grazing was the dominant loss factor of the prokaryotic community, although there was also evidence that viral lysis was occurring. Bermúdez et al. (2016) reported the highest biomass of protozoans around day 15. This was predominantly the heterotrophic choanoflagellate *Calliacantha natans*, which selectively feeds on particles < 1 µm in diameter (Marchant and Scott, 1993; Hornick et al., 2017). Indeed, an earlier study in this area showed that heterotrophic nanoflagellates were the dominant grazers of bacteria responsible for the ingestion of approximately 53 % of bacterial production compared to only 11 % being grazing by ciliates (Uitto et al., 1997). During the first half of Phase II, grazing was reduced and likely contributed to the steady increase in prokaryote abundances. Specifically, a negative relationship between the abundances of HNA prokaryotes and fCO_2 was detected and corresponded to reduced bacterial production and respiration at higher fCO_2 (Hornick et al., 2017; Spilling et al., 2016). Although CO_2 enrichment may not directly affect bacterial growth, a co-occurring global rise in temperature can increase enzyme activities, affecting bacterial production and respiration rates (Piontek et al., 2009; Wohlers et al., 2009; Wohlers-Zöllner et al., 2011). The enhanced bacterial remineralization of organic matter may stimulate autotrophic production by the small-sized phytoplankton (Riebesell et al., 2009; Riebesell and Tortell, 2011; Engel et al., 2013), intensifying the selection of small cell sizes.

Mean viral abundances were higher under CO_2 enrichment towards the end of Phase I and into Phase II, which is expected under conditions of increased phytoplankton and prokaryote biomass. The estimated average viral burst size obtained from this increase in total viral abundance and concurrent decline in bacterial abundances was about 30, which is comparable to published values (Parada et al., 2006; Wommack and Colwell, 2000). Viral lysis rates of prokaryotes were measured until day 25 and indicated that during days 18–25 an average 10–15 % of the total prokaryote population was lysed per day. Moreover, the concurrent steady increase in viral abundances during Phase III indicates that viral lysis of the prokaryotes remained important. Thus, the combined impact of increased viral mortality together with reduced production (Hornick et al., 2017) ultimately led to the decline in prokaryote abundance (this study). Lysogeny did not appear to be an important life strategy of viruses during our campaign. Direct effects of higher fCO_2 on viruses are

not expected, as marine virus isolates are quite stable (both in terms of particle decay and loss of infectivity) over the range of pH in the present study (Danovaro et al., 2011; Mojica and Brussaard, 2014). The few studies which have inferred viral lysis rates based on changes in viral abundances show reduced abundances of algal viruses (e.g. *Emiliania huxleyi*) under enhanced CO_2 (Larsen et al., 2008), while mesocosm results by Brussaard et al. (2013) indicated a stronger impact of viruses on bacterial abundance dynamics with CO_2 enrichment.

5 Conclusions

Due to the low buffering capacity of the Baltic Sea and the paucity of data regarding OA impact in nutrient-limited waters, the results presented here are pertinent to increasing our understanding of how projected rises in fCO_2 will affect the microbial communities in this region. Our study provides evidence that cell size, taxonomy and sensitivity to loss can all play a role in the outcome of CO_2 enrichment. Physiological constraints of cell size favour nutrient uptake by small cells under conditions of reduced nutrients, and our results show that these effects can be further exacerbated by OA. Gross growth rates along with the complementary mortality rates allowed for a more comprehensive understanding of the phytoplankton population dynamics and thus perception of how microbial food web dynamics can influence the response of the autotrophic and heterotrophic components of the community. Our results further suggest that alterations in CO_2 concentrations are expected to affect prokaryote communities (mainly) indirectly through alterations in phytoplankton biomass, productivity and viral lysis. Overall, the combination of growth and losses (grazing and viral lysis) could explain the microbial population dynamics observed in this study. It is noteworthy to mention a recent study in the oligotrophic northeastern Atlantic Ocean, which reported a shift from a grazing-dominated to a viral-lysis-dominated phytoplankton community with strengthening vertical stratification (shoaling the mixed layer depth and enhancing nutrient limitation; Mojica et al., 2016). Thus, we highly recommend that future research on OA combine mesocosm studies focusing on changes in microbial community composition and activity with experiments aimed at understanding the effects of OA on food web dynamics, i.e. partitioning mortality between grazing and viral lysis (Brussaard et al., 2008).

Data availability. Phytoplankton abundance, https://doi.pangaea.de/10.1594/PANGAEA.879659; phytoplankton loss and growth rate, https://doi.pangaea.de/10.1594/PANGAEA.879660; grazing and viral lysis of prokaryotes, https://doi.pangaea.de/10.1594/PANGAEA.879661.

The Supplement related to this article is available online at https://doi.org/10.5194/bg-14-3831-2017-supplement.

Author contributions. Design and overall coordination of research by CB. Organization and performance of analyses in the field by KC. Data analysis by KC, CB and SA-F. Design and coordination of the overall KOSMOS mesocosm project by UR. All authors contributed to the writing of the paper (KC, KM and CB are lead authors).

Competing interests. The authors declare that they have no conflict of interest.

Special issue statement. This article is part of the special issue "Effects of rising CO_2 on a Baltic Sea plankton community: ecological and biogeochemical impacts". It is not associated with a conference.

Acknowledgements. This project was funded through grants to Corina P. D. Brussaard by the Darwin project, the Netherlands Institute for Sea Research (NIOZ) and the EU project MESOAQUA (grant agreement number 228224). We thank the KOSMOS project organizers and team, in particular Andrea Ludwig, the staff of the Tvärminne Zoological Station and the diving team. We give special thanks to Anna Noordeloos, Kirsten Kooijman and Richard Doggen for their technical assistance during this campaign. We also gratefully acknowledge the captain and crew of R/V *Alkor* for their work transporting, deploying and recovering the mesocosms. The collaborative mesocosm campaign was funded by BMBF projects BIOACID II (FKZ 03F06550) and SOPRAN phase II (FKZ 03F0611).

Edited by: Eric Achterberg
Reviewed by: three anonymous referees

References

Aberle, N., Schulz, K. G., Stuhr, A., Malzahn, A. M., Ludwig, A., and Riebesell, U.: High tolerance of microzooplankton to ocean acidification in an Arctic coastal plankton community, Biogeosciences, 10, 1471–1481, https://doi.org/10.5194/bg-10-1471-2013, 2013.

Barcelos e Ramos, J., Biswas, H., Schulz, K. G., LaRoche, J., and Riebesell, U.: Effect of rising atmospheric carbon dioxide on the marine nitrogen fixer *Trichodesmium*, Global Biogeochem. Cy., 21, GB2028, https://doi.org/10.1029/2006GB002898, 2007.

Baudoux, A. C., Noordeloos, A. A. M., Veldhuis, M. J. W., and Brussaard, C. P. D.: Virally induced mortality of *Phaeocystis globosa* during two spring blooms in temperate coastal waters, Aquat. Microb. Ecol., 44, 207–217, https://doi.org/10.3354/ame044207, 2006.

Bermúdez, R., Winder, M., Stuhr, A., Almén, A.-K., Engström-Öst, J., and Riebesell, U.: Effect of ocean acidification on

the structure and fatty acid composition of a natural plankton community in the Baltic Sea, Biogeosciences, 13, 6625–6635, https://doi.org/10.5194/bg-13-6625-2016, 2016.

Brussaard, C. P. D.: Optimization of Procedures for Counting Viruses by Flow Cytometry, Appl. Environ. Microb., 70, 1506–1513, https://doi.org/10.1128/AEM.70.3.1506-1513.2004, 2004.

Brussaard, C. P. D., Kuipers, B., and Veldhuis, M. J. W.: A mesocosm study of *Phaeocystis globosa* population dynamics: I. Regulatory role of viruses in bloom control, Harmful Algae, 4, 859–874, https://doi.org/10.1016/j.hal.2004.12.015, 2005.

Brussaard, C. P. D., Wilhelm, S. W., Thingstad, F., Weinbauer, M. G., Bratbak, G., Heldal, M., Kimmance, S. A., Middelboe, M., Nagasaki, K., Paul, J. H., Schroeder, D. C., Suttle, C. A., Vaqué, D., and Wommack, K. E.: Global-scale processes with a nanoscale drive: the role of marine viruses, ISME J., 2, 575–578, https://doi.org/10.1038/ismej.2008.31, 2008.

Brussaard, C. P. D., Noordeloos, A. A. M., Witte, H., Collenteur, M. C. J., Schulz, K., Ludwig, A., and Riebesell, U.: Arctic microbial community dynamics influenced by elevated CO_2 levels, Biogeosciences, 10, 719–731, https://doi.org/10.5194/bg-10-719-2013, 2013.

Clarke, K. R.: Non-parametric multivariate analyses of changes in community structure, Aust. J. Ecol., 18, 117–143, 1993.

Corno, G., Karl, D., Church, M., Letelier, R., Lukas, R., Bidigare, R., and Abbott, M.: Impact of climate forcing on ecosystem processes in the North Pacific Subtropical Gyre, J. Geophys. Res., 112, C04021, https://doi.org/10.1029/2006JC003730, 2007.

Danovaro, R., Corinaldesi, C., Dell'Anno, A., Fuhrman, J. A., Middelburg, J. J., Noble, R. T., and Suttle, C. A.: Marine viruses and global climate change, FEMS Microbiol. Rev., 35, 993–1034, 2011.

Davidson, A., McKinlay, J., Westwood, K., Thomson, P., Van Den Enden, R., De Salas, M., Wright, S., Johnson, R., and Berry, K.: Enhanced CO_2 concentrations change the structure of Antarctic marine microbial communities, Mar. Ecol.-Prog. Ser., 552, 93–113, https://doi.org/10.3354/meps11742, 2016.

Doney, S. C., Fabry, V. J., Feely, R. A., and Kleypas, J. A.: Ocean acidification: The other CO_2 problem, Annual Review of Marine Science, 1, 169–192, 2009.

Dutkiewicz, S., Morris, J. J., Follows, M. J., Scott, J., Levitan, O., Dyhrman, S. T., and Berman-Frank, I.: Impact of ocean acidification on the structure of future phytoplankton communities, Nature Climate Change, 5, 1002–1006, 2015.

Eberlein, T., Wohlrab, S., Rost, B., John, U., Bach, L. T., Riebesell, U., and Van de Waal, D. B.: Effects of ocean acidification on primary production in a coastal North Sea phytoplankton community, PLoS ONE, 12, e0172594, https://doi.org/10.1371/journal.pone.0172594, 2017.

Engel, A., Schulz, K. G., Riebesell, U., Bellerby, R., Delille, B., and Schartau, M.: Effects of CO_2 on particle size distribution and phytoplankton abundance during a mesocosm bloom experiment (PeECE II), Biogeosciences, 5, 509–521, https://doi.org/10.5194/bg-5-509-2008, 2008.

Engel, A., Borchard, C., Piontek, J., Schulz, K. G., Riebesell, U., and Bellerby, R.: CO_2 increases ^{14}C primary production in an Arctic plankton community, Biogeosciences, 10, 1291–1308, https://doi.org/10.5194/bg-10-1291-2013, 2013.

Evans, C. and Brussaard, C. P. D.: Regional variation in lytic and lysogenic viral infection in the Southern Ocean and its contribution to biogeochemical cycling, Appl. Environ. Microb., 78, 6741–6748, 2012.

Feng, Y., Leblanc, K., Rose, J. M., Hare, C. E., Zhang, Y., Lee, P. A., Wilhelm, S. W., DiTullio, G. R., Rowe, J. M., Sun, J., Nemcek, N., Gueguen, C., Passow, U., Benner, I., Hutchins, D. A., and Brown, C.: Effects of increased pCO_2 and temperature on the North Atlantic spring bloom. I. The phytoplankton community and biogeochemical response, Mar. Ecol.-Prog. Ser., 388, 13–25, https://doi.org/10.3354/meps08133, 2009.

Field, C. B., Behrenfeld, M. J., Randerson, J. T., and Falkowski, P.: Primary Production of the Biosphere: Integrating Terrestrial and Oceanic Components, Science, 281, 237–240, https://doi.org/10.1126/science.281.5374.237, 1998.

Flynn, K. J., Blackford, J. C., Baird, M. E., Raven, J. A., Clark, D. R., Beardall, J., Brownlee, C., Fabian, H., and Wheeler, G. L.: Letter. Changes in pH at the exterior surface of plankton with ocean acidification, Nature Climate Change, 2, 510–513, https://doi.org/10.1038/nclimate1696, 2012.

Fu, F. X., Warner, M. E., Zhang, Y., Feng, Y., and Hutchins, D. A.: Effects of increased temperature and CO_2 on photosynthesis, growth, and elemental ratios in marine *Synechococcus* and *Prochlorococcus* (Cyanobacteria), J. Phycol., 43, 485–496, https://doi.org/10.1111/j.1529-8817.2007.00355.x, 2007.

Garrison, D. L., Gowing, M. M., Hughes, M. P., Campbell, L., Caron, D. A., Dennett, M. R., Shalapyonok, A., Olson, J. A., Landry, M. R., Brown, S. L., Liu, H-B., Azam, F., Steward, G. F., Ducklow, H. W., and Smith, D. C.: Microbial food web structure in the Arabian Sea: A US JGOFS study, Deep-Sea Res. Pt. II, 47, 1387–1422, https://doi.org/10.1016/S0967-0645(99)00148-4, 2000.

Gazeau, F., Sallon, A., Pitta, P., Tsiola, A., Maugendre, L., Giani, M., Celussi, M., Pedrotti, M. L., Marro, S., and Guieu, C.: Limited impact of ocean acidification on phytoplankton community structure and carbon export in an oligotrophic environment: results from two short-term mesocosm studies in the Mediterranean Sea, Estuar. Coast. Shelf S., 186, 72–88, https://doi.org/10.1016/j.ecss.2016.11.016, 2017.

Gruber, N.: Warming up, turning sour, losing breath: Ocean biogeochemistry under global change, Philos. T. Roy. Soc. A, 369, 1980–1996, 2011.

Haverkamp, T., Schouten, D., Doeleman, M., Wollenzien, U., Huisman, J., and Stal, L.: Colorful microdiversity of *Synechococcus* strains (picocyanobacteria) isolated from the Baltic Sea, ISME J., 3, 397–408, 2009.

Hein, M. and Sand-Jensen, K.: CO_2 increases oceanic primary production, Nature, 388, 526–527, 1997.

Hopkins, F. E., Turner, S. M., Nightingale, P. D., Steinke, M., Bakker, D., and Liss, P. S.: Ocean acidification and marine trace gas emissions, P. Natl. Acad. Sci. USA, 107, 760–765, https://doi.org/10.1073/pnas.0907163107, 2010.

Hornick, T., Bach, L. T., Crawfurd, K. J., Spilling, K., Achterberg, E. P., Woodhouse, J. N., Schulz, K. G., Brussaard, C. P. D., Riebesell, U., and Grossart, H.-P.: Ocean acidification impacts bacteria-phytoplankton coupling at low-nutrient conditions, Biogeosciences, 14, 1–15, https://doi.org/10.5194/bg-14-1-2017, 2017.

Hutchins, D. A., Fe, F-X., Zhang, Y., Warner, M. E., Feng, Y., Portune, K., Bernhardt, P. W., and Mulholland, M. R.: CO_2 control of *Trichodesmium* N_2 fixation, photosynthesis, growth rates, and

elemental ratios: implications for past, present, and future ocean biogeochemistry, Limnol. Oceanogr., 52, 1293–1304, 2007.

Jansson, A., Norkko, J., and Norkko, A.: Effects of Reduced pH on *Macoma balthica* Larvae from a System with Naturally Fluctuating pH-Dynamics, PLoS One, 8, e68198, https://doi.org/10.1371/journal.pone.0068198, 2013.

Kimmance, S. A. and Brussaard, C. P. D.: Estimation of viral-induced phytoplankton mortality using the modified dilution method, in: Manual of Aquatic Viral Ecology, edited by: Wilhelm, S. W., Weinbauer, M., and Suttle, C. A., ASLO, 65–73, 2010.

Klaveness, D.: Biology and ecology of the Cryptophyceae: status and challenges, Biological Oceanography, 6, 257–270, 1989.

Kuliński, K. and Pempkowiak, J.: The carbon budget of the Baltic Sea, Biogeosciences, 8, 3219–3230, https://doi.org/10.5194/bg-8-3219-2011, 2011.

Kuosa, H.: Picoplanktonic algae in the northern Baltic Sea: seasonal dynamics and flagellate grazing, Mar. Ecol.-Prog. Ser., 73, 269–276, https://doi.org/10.3354/meps073269, 1991.

Kuosa, H. and Kivi, K.: Bacteria and heterotrophic flagellates in the pelagic carbon cycle in the northern Baltic Sea, Mar. Ecol.-Prog. Ser., 53, 93–100, https://doi.org/10.3354/meps053093, 1989.

Larsen, J. B., Larsen, A., Thyrhaug, R., Bratbak, G., and Sandaa, R.-A.: Response of marine viral populations to a nutrient induced phytoplankton bloom at different pCO_2 levels, Biogeosciences, 5, 523–533, https://doi.org/10.5194/bg-5-523-2008, 2008.

Legendre, P. and Legendre, L.: Numerical Ecology, Elsevier, Amsterdam, New York, 1998.

Lehmann, A. and Myrberg, K.: Upwelling in the Baltic Sea – A review, J. Marine Syst., 74, S3–S12, https://doi.org/10.1016/j.jmarsys.2008.02.010, 2008.

Leonardos, N. and Geider, R. J.: Elevated atmospheric carbon dioxide increases organic carbon fixation by *Emiliania huxleyi* (Haptophyta), under nutrient-limited high-light conditions, J. Phycol., 41, 1196–1203, https://doi.org/10.1111/j.1529-8817.2005.00152.x, 2005.

Lips, I. and Lips, U.: Phytoplankton dynamics affected by the coastal upwelling events in the Gulf of Finland in July–August 2006, J. Plankton Res., 32, 1269–1282, 2010.

Lischka, S., Bach, L. T., Schulz, K.-G., and Riebesell, U.: Ciliate and mesozooplankton community response to increasing CO_2 levels in the Baltic Sea: insights from a large-scale mesocosm experiment, Biogeosciences, 14, 447–466, https://doi.org/10.5194/bg-14-447-2017, 2017.

Lønborg, C., Middelboe, M., and Brussaard, C. P. D.: Viral lysis of Micromonas pusilla: Impacts on dissolved organic matter production and composition, Biogeochemistry, 116, 231–240, https://doi.org/10.1007/s10533-013-9853-1, 2013.

Lu, Z., Jiao, N., and Zhang, H.: Physiological changes in marine picocyanobacterial *Synechococcus* strains exposed to elevated CO_2 partial pressure, Mar. Biol. Res., 2, 424–430, https://doi.org/10.1080/17451000601055419, 2006.

Marchant, H. J. and Scott, F. J: Uptake of sub-micrometre particles and dissolved organic material by Antarctic choanoflagellates, Mar. Ecol.-Prog. Ser., 92, 59–64, 1993.

Marie, D., Brussaard, C. P. D., Thyrhaug, R., Bratbak, G., and Vaulot, D.: Enumeration of marine viruses in culture and natural samples by flow cytometry, Appl. Environ. Microbiol., 65, 45–52, 1999.

Meakin, N. G. and Wyman, M.: Rapid shifts in picoeukaryote community structure in response to ocean acidification, ISME J., 5, 1397–405, https://doi.org/10.1038/ismej.2011.18, 2011.

Meyer, J. and Riebesell, U.: Reviews and Syntheses: Responses of coccolithophores to ocean acidification: a meta-analysis, Biogeosciences, 12, 1671–1682, https://doi.org/10.5194/bg-12-1671-2015, 2015.

Middelboe, M. and Lyck, P. G.: Regeneration of dissolved organic matter by viral lysis in marine microbial communities, Aquat. Microb. Ecol., 27, 187–194, https://doi.org/10.3354/ame027187, 2002.

Mojica, K. D. A. and Brussaard, C. P. D.: Factors affecting virus dynamics and microbial host–virus interactions in marine environments, FEMS Microbiol. Ecol., 89, 495–515, https://doi.org/10.1111/1574-6941.12343, 2014.

Mojica, K. D. A., Evans, C., and Brussaard, C. P. D.: Flow cytometric enumeration of marine viral populations at low abundances, Aquat. Microb. Ecol., 71, 203–209, https://doi.org/10.3354/ame01672, 2014.

Mojica, K. D. A., Huisman, J., Wilhelm, S. W., and Brussaard, C. P. D.: Latitudinal variation in virus-induced mortality of phytoplankton across the North Atlantic Ocean, ISME J., 10, 500–513, https://doi.org/10.1038/ismej.2015.130, 2016.

Motwani, N. H. and Gorokhova, E.: Mesozooplankton grazing on picocyanobacteria in the Baltic Sea as inferred from molecular diet analysis, PLoS ONE, 8, e79230, https://doi.org/10.1371/journal.pone.0079230, 2013.

Niehoff, B., Schmithüsen, T., Knüppel, N., Daase, M., Czerny, J., and Boxhammer, T.: Mesozooplankton community development at elevated CO_2 concentrations: results from a mesocosm experiment in an Arctic fjord, Biogeosciences, 10, 1391–1406, https://doi.org/10.5194/bg-10-1391-2013, 2013.

Nõmmann, S., Sildam, J., Nõges, T., and Kahru, M.: Plankton distribution during a coastal upwelling event off Hiiumaa, Baltic Sea: impact of short-term flow field variability, Cont. Shelf Res., 11, 95–108, 1991.

Oksanen, J., Blanchet, F. G., Friendly, M., Kindt, R., Legendre, P., McGlinn, D., Minchin, P., R., O'Hara, R. B., L. Simpson, G. L., Solymos, P., Stevens, M. H. H., Szoecs, E., and Wagner, H.: vegan: Community Ecology Package, R package version 2.4-3, available at: https://CRAN.R-project.org/package=vegan, 2017.

Parada, V., Herndl, G., and Weinbauer, M.: Viral burst size of heterotrophic prokaryotes in aquatic systems, J. Mar. Biol. Assoc. UK, 86, 613–621, https://doi.org/10.1017/S002531540601352X, 2006.

Paul, A. J., Bach, L. T., Schulz, K.-G., Boxhammer, T., Czerny, J., Achterberg, E. P., Hellemann, D., Trense, Y., Nausch, M., Sswat, M., and Riebesell, U.: Effect of elevated CO_2 on organic matter pools and fluxes in a summer Baltic Sea plankton community, Biogeosciences, 12, 6181–6203, https://doi.org/10.5194/bg-12-6181-2015, 2015.

Paulino, A. I., Egge, J. K., and Larsen, A.: Effects of increased atmospheric CO_2 on small and intermediate sized osmotrophs during a nutrient induced phytoplankton bloom, Biogeosciences, 5, 739–748, https://doi.org/10.5194/bg-5-739-2008, 2008.

Pfeil, B., Olsen, A., Bakker, D. C. E., Hankin, S., Koyuk, H., Kozyr, A., Malczyk, J., Manke, A., Metzl, N., Sabine, C. L., Akl, J., Alin, S. R., Bates, N., Bellerby, R. G. J., Borges, A., Boutin, J., Brown, P. J., Cai, W.-J., Chavez, F. P., Chen, A., Cosca, C.,

Fassbender, A. J., Feely, R. A., González-Dávila, M., Goyet, C., Hales, B., Hardman-Mountford, N., Heinze, C., Hood, M., Hoppema, M., Hunt, C. W., Hydes, D., Ishii, M., Johannessen, T., Jones, S. D., Key, R. M., Körtzinger, A., Landschützer, P., Lauvset, S. K., Lefèvre, N., Lenton, A., Lourantou, A., Merlivat, L., Midorikawa, T., Mintrop, L., Miyazaki, C., Murata, A., Nakadate, A., Nakano, Y., Nakaoka, S., Nojiri, Y., Omar, A. M., Padin, X. A., Park, G.-H., Paterson, K., Perez, F. F., Pierrot, D., Poisson, A., Ríos, A. F., Santana-Casiano, J. M., Salisbury, J., Sarma, V. V. S. S., Schlitzer, R., Schneider, B., Schuster, U., Sieger, R., Skjelvan, I., Steinhoff, T., Suzuki, T., Takahashi, T., Tedesco, K., Telszewski, M., Thomas, H., Tilbrook, B., Tjiputra, J., Vandemark, D., Veness, T., Wanninkhof, R., Watson, A. J., Weiss, R., Wong, C. S., and Yoshikawa-Inoue, H.: A uniform, quality controlled Surface Ocean CO_2 Atlas (SOCAT), Earth Syst. Sci. Data, 5, 125–143, https://doi.org/10.5194/essd-5-125-2013, 2013.

Pinheiro, J., Bates, D., DebRoy, S., Sarkar, D., and R Core Team: nlme: Linear and Nonlinear Mixed Effects Models, R package version 3.1-131, available at: https://CRAN.Rproject.org/package=nlme, 2017.

Piontek, J., Händel, N., Langer, G., Wohlers, J., Riebesell, U., and Engel, A.: Effects of rising temperature on the formation and microbial degradation of marine diatom aggregates, Aquat. Microb. Ecol., 54, 305–318, https://doi.org/10.3354/ame01273, 2009.

Qiu, B. and Gao, K.: Effects of CO_2 enrichment on the bloom-forming cyanobacterium *Microcystis aeruginosa* (Cyanophyceae): Physiological responses and relationships with the availability of dissolved inorganic carbon, J. Phycol., 38, 721–729, https://doi.org/10.1046/j.1529-8817.2002.01180.x, 2002.

R Core Team: R: A language and environment for statistical computing, R Foundation for Statistical Computing, Vienna, Austria, available at: https://www.R-project.org/, 2017.

Raven, J. A.: The twelfth Tansley Lecture. Small is beautiful: the picophytoplankton, Funct. Ecol., 12, 503–513, https://doi.org/10.1046/j.1365-2435.1998.00233.x, 1998.

Riebesell, U., Körtzinger, A., and Oschlies, A.: Sensitivities of marine carbon fluxes to ocean change, P. Natl. Acad. Sci. USA, 106, 20602–20609, https://doi.org/10.1073/pnas.0813291106, 2009.

Riebesell, U. and Tortell, P. D.: Effects of ocean acidification on pelagic organisms and ecosystems, in: Ocean acidification, edited by: Gattuso, J.-P. and Hansson, L., Oxford University Press, Oxford, UK, 99–121, 2011.

Riebesell, U., Czerny, J., von Bröckel, K., Boxhammer, T., Büdenbender, J., Deckelnick, M., Fischer, M., Hoffmann, D., Krug, S. A., Lentz, U., Ludwig, A., Muche, R., and Schulz, K. G.: Technical Note: A mobile sea-going mesocosm system – new opportunities for ocean change research, Biogeosciences, 10, 1835–1847, https://doi.org/10.5194/bg-10-1835-2013, 2013.

Riebesell, U., Bach, L. T., Bellerby, R. G. J., Bermudez, R., Boxhammer, T., Czerny, J., Larsen, A., Ludwig, A., and Schulz, K. G.: Ocean acidification impairs competitive fitness of a predominant pelagic calcifier, Nat. Geosci., 10, 19–24, https://doi.org/10.1038/ngeo2854, 2017.

Rose, J. M., Feng, Y., Gobler, C. J., Gutierrez, R., Harel, C. E., Leblancl, K., and Hutchins, D. A.: Effects of increased pCO_2 and temperature on the North Atlantic spring bloom. II. Microzooplankton abundance and grazing, Mar. Ecol.-Prog. Ser., 388, 27–40, https://doi.org/10.3354/meps08134, 2009.

Schaum, E., Rost, B., Millar, A. J., and Collins, S.: Variation in plastic responses of a globally distributed picoplankton species to ocean acidification, Nature Climate Change, 3, 298–302, https://doi.org/10.1038/nclimate1774, 2012.

Schulz, K. G. and Riebesell, U.: Diurnal changes in seawater carbonate chemistry speciation at increasing atmospheric carbon dioxide, Mar. Biol., 160, 1889–1899, https://doi.org/10.1007/s00227-012-1965-y, 2013.

Schulz, K. G., Bach, L. T., Bellerby, R. G. J., Bermúdez, R., Büdenbender, J., Boxhammer, T., Czerny, J., Engel, A., Ludwig, A., Meyerhöfer, M., Larsen, A., Paul, A. J., Sswat, M., and Riebesell, U.: Phytoplankton Blooms at Increasing Levels of Atmospheric Carbon Dioxide: Experimental Evidence for Negative Effects on Prymnesiophytes and Positive on Small Picoeukaryotes, Frontiers in Marine Science, 4, 64, https://doi.org/10.3389/fmars.2017.00064, 2017.

Sheik, A. R., Brussaard, C. P. D., Lavik, G., Lam, P., Musat, N., Krupke, A., Littmann, S., Strous, M., and Kuypers, M. M. M.: Responses of the coastal bacterial community to viral infection of the algae Phaeocystis globosa, ISME J., 8, 212–25, https://doi.org/10.1038/ismej.2013.135, 2014.

Sherr, E. B., Caron, D. A., and Sherr, B. F.: Staining of heterotrophic protists for visualization via epifluorescence microscopy, in: Current Methods in Aquatic Microbial Ecology, edited by: Sherr, B., Sherr, E., and Kemp, J. C. P., Lewis Publ., NY, 213–228, 1993.

Spilling, K., Paul, A. J., Virkkala, N., Hastings, T., Lischka, S., Stuhr, A., Bermúdez, R., Czerny, J., Boxhammer, T., Schulz, K. G., Ludwig, A., and Riebesell, U.: Ocean acidification decreases plankton respiration: evidence from a mesocosm experiment, Biogeosciences, 13, 4707–4719, https://doi.org/10.5194/bg-13-4707-2016, 2016.

Stoecker, D. K., Nejstgaard, J., Madhusoodhanan, R., and Larsen, A.: Underestimation of microzooplankton grazing in dilution experiments due to inhibition of phytoplankton growth, Limnol. Oceanogr., 60, 1426–1438, https://doi.org/10.1002/lno.10106, 2015.

Suffrian, K., Simonelli, P., Nejstgaard, J. C., Putzeys, S., Carotenuto, Y., and Antia, A. N.: Microzooplankton grazing and phytoplankton growth in marine mesocosms with increased CO_2 levels, Biogeosciences, 5, 1145–1156, https://doi.org/10.5194/bg-5-1145-2008, 2008.

Tortell, P. D., DiTullio, G. R., Sigman, D. M., and Morel, F. M. M.: CO_2 effects on taxonomic composition and nutrient utilization in an Equatorial Pacific phytoplankton assemblage, Mar. Ecol.-Prog. Ser., 236, 37–43, 2002.

Traving, S. J., Clokie, M. R. J., and Middelboe, M.: Increased acidification has a profound effect on the interactions between the cyanobacterium *Synechococcus* sp. WH7803 and its viruses, FEMS Microbiol. Ecol., 87, 133–141, https://doi.org/10.1111/1574-6941.12199, 2014.

Turley, C. and Boot, K.: UNEP emerging issues: Environmental consequences of ocean acidification: A threat to food security, United Nations Environment Programme, 2010.

Uitto, A., Heiskanen, A., Lignell, R., Autio, R., and Pajuniemi, R.: Summer dynamics of the coastal planktonic food web in the northern Baltic Sea, Mar. Ecol.-Prog. Ser., 151, 27–41, https://doi.org/10.3354/meps151027, 1997.

Veldhuis, M. J. W. and Kraay, G. W.: Phytoplankton in the subtropical Atlantic Ocean: Towards a better assessment of

biomass and composition, Deep-Sea Res. Pt I, 51, 507–530, https://doi.org/10.1016/j.dsr.2003.12.002, 2004.

Veldhuis, M. J. W., Timmermans, K. R., Croot, P., and Van Der Wagt, B.: Picophytoplankton; A comparative study of their biochemical composition and photosynthetic properties, J. Sea Res., 53, 7–24, https://doi.org/10.1016/j.seares.2004.01.006, 2005.

Weinbauer, M. G.: Ecology of prokaryotic viruses, FEMS Microbiol. Rev., 28, 127–181, https://doi.org/10.1016/j.femsre.2003.08.001, 2004.

Weinbauer, M. G. and Suttle, C. A.: Potential significance of lysogeny to bacteriophage production and bacterial mortality in coastal waters of the Gulf of Mexico, Appl. Environ. Microb., 62, 4374–4380, 1996.

Weinbauer, M. G., Mari, X., and Gattuso, J.-P.: Effect of ocean acidification on the diversity and activity of heterotrophic marine microorganisms, in: Ocean Acidification, edited by: Gattuso, J.-P. and Hansson, L., Oxford University Press, Oxford, UK, 83–98, 2011.

Wilhelm, S. W. and Suttle, C. A.: Viruses and Nutrient Cycles in the Sea aquatic food webs, BioScience, 49, 781–788, https://doi.org/10.2307/1313569, 1999.

Wilhelm, S. W., Brigden, S. M., and Suttle, C. A.: A dilution technique for the direct measurement of viral production: A comparison in stratified and tidally mixed coastal waters, Microb. Ecol., 43, 168–173, https://doi.org/10.1007/s00248-001-1021-9, 2002.

Winget, D. M., Williamson, K. E., Helton, R. R., and Wommack, K. E.: Tangential flow diafiltration: An improved technique for estimation of virioplankton production, Aquat. Microb. Ecol., 41, 221–232, https://doi.org/10.3354/ame041221, 2005.

Wohlers, J., Engel, A., Zöllner, E., Breithaupt, P., Jürgens, K., Hoppe, H.-G., Sommer, U., and Riebesell, U.: Changes in biogenic carbon flow in response to sea surface warming, P. Natl. Acad. Sci. USA, 106, 7067–7072, https://doi.org/10.1073/pnas.0812743106, 2009.

Wohlers-Zöllner, J., Breithaupt, P., Walther, K., Jürgens, K., and Riebesell, U.: Temperature and nutrient stoichiometry interactively modulate organic matter cycling in a pelagic algal-bacterial community, Limnol. Oceanogr., 56, 599–610, https://doi.org/10.4319/lo.2011.56.2.0599, 2011.

Wolf-Gladrow, D. and Riebesell, U.: Diffusion and reactions in the vicinity of plankton: A refined model for inorganic carbon transport, Mar. Chem., 59, 17–34, https://doi.org/10.1016/S0304-4203(97)00069-8, 1997.

Wommack, K. E. and Colwell, R. R.: Virioplankton: viruses in aquatic ecosystems, Microbiol. Mol. Biol. R., 64, 69–114, 2000.

Worden, A. Z., Nolan, J. K., and Palenik, B.: Assessingthe dynamics and ecology of marine picophytoplankton: The importance of the eukaryotic component, Limnol. Oceanogr., 49, 168–179, https://doi.org/10.4319/lo.2004.49.1.0168, 2004.

Zuur, A. F., Ieno, E. N., and Smith, G. M.: Analysing Ecological Data, in: Statistics for Biology and Health, Springer, New York, https://doi.org/10.1007/978-0-387-45972-1, 2007.